Dr. Sebastian D. Eastham
Research Scientist
Department of Aeronautics and Astronautics
Laboratory for Aviation and the Environment

Massachusetts Institute of Technology
77 Mass. Ave. Office 33-322A, Cambridge MA 02139, USA
seastham@mit.edu | http://lae.mit.edu | +1 617–452–2550

Editorial Office
Atmospheric Chemistry and Physics

July 31st, 2020

Dear Editor,

Re: Submission of "Effect of contrail overlap on radiative impact attributable to aviation contrails" to *Atmospheric Chemistry and Physics*

Thank you for arranging the review of our work. We thank the reviewers for their time and attention, and in particular for their comments regarding additional pertinent literature and for their suggestions regarding the paper's structure. We have now incorporated a deeper literature review, and have significantly restructured the paper to more clearly reflect the goals and novelty of the work. This includes the separation of the "Introduction" section into two components: Section 1, which motivates the work and explains our approach; and Section 2, which is now dedicated to providing a thorough overview of previous contributions in this field, and distinguishing our approach (and objectives) from theirs.

Please find below our responses to the comments from anonymous reviewers #1 and #2, as well as to the comment from Michael Ponater. In the responses below, we have listed the reviewer's comments in *italics* and our responses in **bold**. All line numbers refer to the revised manuscript. A marked up copy is attached.

Anonymous Referee #1

The paper discusses the impact of overlap of contrails with other clouds and of contrails with other contrails for horizontally homogeneous clouds and contrails.

The paper offers a simplified radiative transport model to account for RF changed for overlapping cloud layers.

The main conclusions are:

1) *Contrail-cloud overlap is important. Contrails over clear sky and contrails over other clouds have far different radiative forcings (RF).*

True. However, that finding is not surprising and not new. It is not surprising because the clouds below and above contrails change the reflected solar radiation (local Earth albedo) and the outgoing longwave radiation. It is not new since you find that in several previous papers. See, for example Fig. 6, column 6, in Meerkötter et al. (1999; cited in the paper). That paper discussed the sensitivity of RF to various contrail and ambient parameters, including a cloud layer below the contrail cirrus and the optical depth of "background clouds". It showed that the net RF can increase from close to zero to a large positive value when background clouds get included. The value (94%) stated in the present paper here has no significance because it depends on the reference value and may vary from minus infinity to plus infinity when the net RF happens to be close to zero for the reference case considered. That makes no sense.
We agree that the phrasing of a 94% change was misleading in the context of an RF which is the result of changes in two components of different sign. Upon reflection we have changed the way that this is presented, providing information on the effect for both longwave and shortwave components in the abstract (lines 26-27) and conclusions (lines 1056) instead.

The present paper mentions Minnis et al (1999, cited) and Myhre et al. (2009, cited) and other studies, who discussed contrail-cloud overlap. The abstract and conclusions stress the importance and uncertainties of contrail-cloud overlap, which is correct, but report the findings as if that would be new, which is not correct. Apparently, this discussion still reflects the history of the present paper, which apparently started with the Corti-

Peters model with just one cloud layer (contrails or cirrus) over Earth surface and where the inclusion of other clouds changed the results considerably. This needs to be fully revised.
Based on the insights provided by all reviewers and commenters, we realized that the objectives of the paper were not written sufficiently clearly, and that the literature review did not do justice to the existing work in this field. We have therefore heavily reworked the introduction, splitting it into two sections as described in the opening text of this letter.

With regards to this specific comment, we have made a particular effort to clarify the novelty of this paper. We now separate out our motivation, including the specific aims of this work, in a dedicated Section 1. This is followed by a dedicated discussion of previous work on cloud-contrail overlaps (see Section 2.1) in addition to the approaches taken to account for contrail-contrail overlap in previous work, where relevant.

2) *Contrail-contrail overlap depends on the number and proximity of contrails. For present traffic, contrail-contrail overlap occurs on average over the globe but only rarely. This overlap may occur more frequently for increased traffic and under special flight track conditions.*

The treatment of contrail-contrail overlap is interesting. In areas with dense traffic, many contrails overlap with each other and with other clouds to different degrees. It would be good to have an efficient and still accurate method to account for the climate impact of contrails in such situation.
Contrail-contrail overlap may not be the most important uncertainty in contrail RF modelling. More important parameters may include the amount of ice supersaturation available in the atmosphere, the growth of the contrail cross-section by mixing with ambient air and the life time of contrails depending on many parameters (Schumann and Heymsfield, 2017, cited, and the references cited therein). Still, an investigation of contrail-contrail overlap effects and their modelling is of interest.

We agree with the reviewer that while this is a useful new possibility, it is certainly not the only (or even dominant) uncertainty in contrail modeling. We have made a renewed attempt to distinguish between physical uncertainties such as in available ice supersaturation or contrail ice microphysics (lines 69-71); modeling challenges such as the dependence of contrail-attributable radiative forcing on the representation of cloud-contrail overlap; and the unquantified effects of contrail-contrail overlap (lines 79-89).

Comments on the approach and results:

The radiative transfer model used to account for multiple layers (Section 2.1.3) looks interesting. It seems to have similarities with older theories; see, e.g., Hansen and Travis (1974) and Minnis et al. (1993); Minnis et al. (1998). A paper much cited in this respect is that of Ritter and Geleyn (1992). This part needs review by experts in this specfic field.

Section 3.1.4 compares results for this model with the Fu&Liou model. That is certainly an acceptable approach, as long as one can justify the plane-parallel cloud representation. Only few details are given on how the code was applied, for example with respect to the background atmosphere and aerosols and the specific model parameters. The comparison shows qualitative agreements with the multilayer model derived, but significant quantitative differences. So, how can we be sure that the results are correct? So uncertainties remain.
Additional data have been added with regards to the experiment implementation and design (lines 703-711). We also now have a discussion emphasizing the variation of the error with solar zenith angle (lines 729-731). We have also expanded our discussion regarding how differences between our results and those using FL96 might propagate to our results (lines 948-954).

Eq. (3) needs a bit more discussion: As it is written, this equation does not guarantee that RF_LW is positive. How often are negative values occurring?
We now clarify this on lines 346-348. As in Schumann et al. (2012), we treat negative values of RF_{LW} as being equal to zero.

Is Eq. (9) correct? 360? is that 360◦ (2 pi)?
This equation has been changed to instead use radians as suggested.

The discussion of the range of optical depth values (tau below 0.3) might be reasonable for global mean value, but locally the variability can be far larger (Atlas and Wang 2010).

This is correct. Our core results evaluate the impact of contrails with optical depths up to 0.5, at the upper end of contrails modeled by CERM. However we recognize that this does not cover the full range of possibilities. We have therefore generated alternative versions of Figures 2 and 3, showing results for contrail optical depths of up to 1.5 – potentially representative of more contrail-dense areas like Northern America or Europe. These figures can be found in the SI (Figures S3 and S4).

The paper presents contrail results from the model CERM. As stated, CERM does not account for contrail orientation and does not account for contrail position in a grid cell. How can one compute the contrail-contrail overlap effects without knowing the degree of overlap? The mentioned model CoCiP includes such geometry in more detail.
We apologize for the confusion on this point, and have modified the paper's introduction to clarify. As noted by the reviewer, the lack of orientation information from CERM is a limitation of this work, which we now discuss in Section 5. Accordingly, we assume maximum overlap between contrails, providing an upper bound on the effect of contrail-contrail impact with regards to radiative forcing. However, we agree that it would be an important improvement to either modify CERM to report orientation or to use results from a model such as CoCiP which already includes this data. We now state as much on lines 972-979.

How good do the meteorological data used represent humidity? Which time period is covered by the data, what is the spatial and temporal resolution of the data, and what is the vertical resolution in meters near the mean flight level height (around 10 to 12 km asl)? What is the fraction of ice supersaturated air masses in these data and how does this compare to published findings.
CERM uses a resolution of ~350 m at flight altitudes, but uses meteorological data from GEOS-FP which is provided at a slightly coarser resolution of ~500m at flight altitudes. We have an additional paper in preparation which assesses the magnitude of errors in relative humidity as calculated by GEOS, but this is out of the scope of this paper. We do however now mention known issues with relative humidity estimates in reanalysis (lines 1001-1005) including the possibility of a consistent humidity bias in reanalysis data (Jiang et al., 2015; Davis et al., 2017).

I assume, the model uses gridded emission source rates as provided by the FAA's Aviation Environmental Design Tool, but the paper gives no details on this. Are these data accessible to the community? Otherwise the results cannot be checked by other scientists.
We apologize for the oversight, and have added a sentence detailing the source of aircraft emissions data for this work on lines 399-400. Although CERM has previously been used with AEDT, we chose to instead use flight track data estimated by the Aviation Environment Inventory Code (AEIC) for this work (Simone et al., 2013). AEIC is an open-source tool, enabling independent validation of our results.

Very little is said about the satellite data CERES. The paper cites NASA Langley Research Center Atmospheric Science Data Center 2015 as reference and says that the data are provided at three-hour intervals. How can one derive hourly average values from 3-hourly data? How well do they represent the diurnal cycle and how sensitive are they to cirrus clouds and to geometrically thin contrails? How uniform is this sensitivity spatially and temporally, e.g. over land and oceans?
We now provide additional detail regarding the CERES satellite data on lines 447-473. As stated, CERES provides data once very three hours, and we assume constant cloud coverage over this period. Data are provided on a 1° by 1° global grid. We also discuss the likelihood of double-counting (i.e. contrails being observed by CERES while also being simulated by CERM) on lines 479-486. Sensitivity fo thin contrails depends on visibility thresholds. General visibility thresholds have been discussed lately and a common value is an optical depth of 0.05 (Kärcher et al., 2009), while a specific reference on MODIS instrument (used for CERES) mentions thresholds around 0.02 (Dessler and Yang, 2003). This is now mentioned in line 460-467.

The paper says that the "CERES instruments observe both contrails and natural cirrus clouds". I assume this means that CERES provides information only on the sum of contrails and other clouds. That should be clarified.
Correct. This is now clarified on lines 470-471.

The conclusion claims that the results "help to inform policymakers and researchers to identify technical, operational, and regulatory means to reduce these impacts." I think, based on the information given, the paper is still quite far away from this goal.
Based on this comment and those from other reviewers, we have decided to remove this conclusion.

The conclusion "The radiative forcing attributable to a contrail layer increases by a factor of three due to the presence of natural clouds on a global mean basis, but this varies by region" could be formulated inversely, e.g. "if

a model would ignore other clouds the results could be wrong by a factor of three", but the conclusion should also make clear that this is not state of the art. Other models do account for ambient clouds.
We agree that the previous framing was unclear regarding the goals of the paper, while also not providing enough context regarding the depth of existing literature. With that in mind, we now provide a dedicated discussion regarding our contribution on the aspect of cloud-contrail overlap – specifically, to provide a quantitative analysis of the factors which contribute to and determine the magnitude of the effect that clouds have on contrail radiative forcing (lines 73-84). We also reiterate this point in the conclusions (lines 1026-1029).

In the abstract, the growth rate of air traffic is cited. I agree, growth rates of 4.5 % each year over the next 20 years have been estimated in the past by industry, as cited. However, such trend values have large uncertainty and I would recommend omitting such uncertain values from the abstract.
We have removed this statement from the abstract as suggested.

Unfortunately, the paper is not really clear and understandable and the conclusions are overselling the findings. The subject of the paper and some of the results are interesting but the approach and its presentation require major improvements.

I suggest splitting the paper into two parts: One on radiation transfer and one on the application. The first one should describe the model for the impact of cloud overlap on radiative forcing as a purely technical paper, with full validation. That paper should be reviewed by radiation transfer modelling experts. The other paper might then deal with the consequences of contrail-contrail overlap for climate forcing of aviation, addressing the corresponding community.
We hope that the reviewer finds that the revised structure of the paper is clearer, and more accurately conveys our intended message. We also hope that findings are no longer oversold. We believe that these revisions have helped to make a more coherent paper which is best packaged as a single unit, as the technical work (extending the Corti and Peter (2009) model to include multiple layers) was performed with the specific goal of enabling this comparison.

Anonymous Referee #2

The paper investigates the impact of cloud-contrail and contrail-contrail overlap on the radiative forcing due to contrail cirrus. The authors use a radiative transfer model of Corti and Peter that they modify in order to study the impact of cloud overlap on contrail radiative forcing. They consider two options no overlap and maximum overlap and study the difference when using those two assumptions. Cloud and contrail properties are varied systematically and the impact on LW and SW RF is analyzed. Cloud properties are prescribed using observed natural clouds (from Satellite) and CERM simulated contrails. Whereas, in principal the impact of cloud overlap is an interesting topic, the authors' extreme assumptions (no or maximum overlap) limit the relevance of the paper. They wrongly claim that other studies assume no or maximum overlap between contrails and clouds and contrails and contrails and claim that the sensitivity that they see is a measure for the bias of contrail cirrus RF published in the literature. Relevant literature that discusses the impact of overlap on RF in detail has not been discussed and comparisons with the results in the literature only partly made.

We agree that the treatment of literature in the previous version of this paper was insufficient. We have now dramatically expanded the literature review into a separate section (Section 2). This includes a dedicated review of previous attempts to quantify cloud-contrail overlap (Section 2.1) as well as the approaches used in other models to account for contrail-contrail overlap (Section 2.2).

I suggest presenting the work as a sensitivity study, including a detailed comparison with the many results in the literature and removing text stating that the present work improves contrail RF estimates and estimates the uncertainty in contrail RF in the literature or that the results help to inform policymakers and similar claims.

We have now softened our statements regarding policy applicability, including the removal of a sentence identified by Reviewer #1 as problematic in the conclusions. We have also worked to reframe the paper so that its objectives are clearer: to provide a first quantification of the effects of contrail-contrail overlap on net contrail radiative forcing, and to quantitatively investigate the relationship between physical parameters and the effect of contrail overlap (with natural or artificial clouds) on estimated contrail radiative forcing.

Major comments:

1. *The sensitivity of contrail RF on the overlap analyzed in this paper is not a measure for the uncertainty in contrail RF in the literature. Both assumptions used in this paper, no or maximum overlap, are very extreme whereas in the literature mostly maximum random overlap for contrail-cloud and contrail-contrail overlap has been used. The statements that in the literature mainly maximum overlap has been used (e.g. line 346- 348) or that random overlap has been used for contrail-contrail overlap (line 350) the authors partly contradict their own table 1.*

This comment was very useful in directing our thoughts regarding uncertainty. We agree fully that what is being addressed here is not uncertainty so much as a previously unquantified component of contrail radiative forcing, and one where prior estimates of contrail radiative forcing had differed in their treatement. We have rephrased our study (Section 1) and have also separated out the previous treatments of contrail-contrail overlap (Table 2).

2. *The estimate for contrail RF is not an improved estimate relative to the estimates in the literature*

We agree that this is not the purpose of this paper and have removed such claims from the text.

a. *Neither maximum nor no overlap are good assumptions. Maximum overlap is certainly an upper bound for the overlap but far away from the truth.*

We agree with this assessment. The purpose of the paper is to provide a quantitative estimate of 1) the effect that variations in key parameters (e.g. location, season) have on the effect of multi-layer overlap with regards to contrails; and 2) a quantitative assessment of the potential impact that contrail-contrail overlap might have on contrail RF. Since the CERM simulation does not provide contrail orientation (line 407-412), we instead quantify an upper bound using the maximum overlap assumption. This is now explicitly stated in the limitations section (lines 971-979).

b. *Using only cloud data with 3 hourly temporal resolution does not allow for a realistic representation of contrail-cloud overlap or a realistic estimation of overlap frequencies. The low temporal resolution cannot resolve the correlation between cloud and contrail frequency.*

We have added this to our section on limitations (line 989). Although CERES is a state-of-the-science observational product, we agree that its low temporal resolution will bias estimates of the effects of cloud-contrail overlap. Since we also find other limitations associated with the use of CERES data, we have listed the identification of alternative approaches to incorporate natural cloud data as a high priority for future work (lines 1015-1019).

c. *Overlap assumptions have been shown to be dependent on vertical resolution. Even if vertically extended clouds are assumed the vertical overlap decreases strongly with layer depth. When levels are separated by more than 4km the overlap is essentially random (Hogan and Illingworth, 2000). At a low vertical resolution random overlap is a good assumption while maximum overlap is realistic (for vertically extended clouds) at high vertical resolution. At lower horizontal resolution the arguments must include a discussion of synoptic situations and the resulting vertical and horizontal statistics of the moisture field. Using observed cloud statistics aggregated in only 4 atmospheric layers and calculating the overlap with contrails the assumption of maximum overlap is far from realistic.*

We agree that vertical resolution is an important factor, for multiple reasons. Although CERM is capable of simulating the formation and trajectory of contrails at essentially arbitrary vertical resolution, it is limited by the vertical resolution of the moisture field as simulated by the meteorological data (in our case GEOS-FP data have a resolution of approximately 500 m at flight altitudes). The coverage data used in this work, generated by CERM, have a vertical resolution of approximately 350 m at flight altitudes, by interpolating RH and temperature from GEOS-FP. As for the issue of the vertical resolution of clouds, we are grateful to the reviewer for pointing out the assessment by Hogan and Illingworth, which we now cite as part of a discussion of this issue on line 991. We state there that, although a flawed assumption, we believe that maximum overlap is still the most appropriate approach to estimate an upper bound on contrail overlap impacts. However we fully agree that an assessment which prioritizes a more nuanced description of layer overlap, including higher vertical and temporal resolution of natural cloud data, should be prioritized for future work (line 1015).

d. *Assuming maximum overlap between contrails and contrails is not realistic. Even if planes would follow each other on the same flight track advection would mean that contrails don't maximally overlap. But this*

topic does not seem to be very promising as contrails have a low optical depth and the overlap between contrails does not impact the radiative forcing strongly.

It is true that planes following each other on the same flight path would not be expected to produce overlapping contrails, but patches of overlapping contrail are frequently observed in satellite imagery (e.g. Minnis et al., 2011) and model estimates (e.g. Figure 9). However, we realize that our goal of finding an upper bound on this effect is not clearly enough stated, and have made efforts to clarify this throughout the manuscript.

e. *As the authors say whether a contrail cools or warms depends on the height of the clouds that may be vertically overlapping this contrail. The cloud height cannot be properly represented using cloud observations aggregated on only 4 levels.*

As discussed in the prior responses, we have extended our discussion of the limitations associated with use of the CERES natural cloud observations (lines 989-995 and 1015-1019).

3. *Comparison of the results to the previous publications should be improved.*

a. *The publications of Markowicz and Witek (2011 a,b) have not be cited. They discuss the impact of contrail cloud overlap in great detail e.g. the dependence on particle habit. They also show that contrail RF turns negative for all considered ice crystal shapes at much higher optical depth (at zenith angle 30◦) then shown in fig. 3a. As a zenith angle of 30◦ is often used in the literature it would be good to supply results for that angle in order to allow for comparison.*

These references are now cited in Table 2 and Section 2.1. We have also regenerated Figures 2 to 5 using a solar zenith angle of 30° and added them to the supplementary information (Figures S3, S6, S7 and S8).

b. *The results in Fig. 7 should be compared with results of e.g. Schumann et al. 2012 and Myhre et al 2009 in detail. Why are absolute values of contrail RF so different from previous results?*

This comparison is included on lines 760-765. The resulting global sensitivity in all-sky conditions is of the same order as previous estimates (~100 mW/m^2). The differences in clear-sky results might be due to the assumed asymmetry parameter, with a significant impact on global longwave radiative forcing in clear-sky conditions (Sanz-Morère et al. 2020).

4. *The result that cloud-contrail overlap is responsible for 93% of the net radiative forcing attributable to contrails in 2015 relies on the assumption that the authors have simulated the 'true' overlap between contrails and natural clouds which is not the case. Instead they should say that overlapping contrails maximally with clouds instead of prescribing no overlap leads to an increase in radiative forcing by xx%. The same is true for the statements about the importance of contrail-contrail overlap. Note also that those values will be resolution dependent so that their significance is very limited and should not appear in the abstract!*

We agree that this is misleading. We've removed the statement in question, instead providing the contribution to longwave and shortwave individually which should be more robust. We have also made this modification throughout the paper (e.g. lines 854-855).

5. *Line 891-892: How do you suggest avoiding cloud contrail overlap? Contrails mostly form close to natural clouds which means that they often overlap with other clouds. Cloud-free areas are mostly dry and therefore persistent contrails cannot exist.*

There have been several studies of possible contrail avoidance strategy which may be pertinent here, including recently by Teoh et al (2020). This suggests that, if high-accuracy meteorological data are available, it may be possible to avoid contrails through altitude adjustments. However, we do agree that contrail avoidance is a non-trivial task, and have added this caveat on line 1050.

Minor comments:

1. Table 1 is incomplete, contains mistakes and is misleading: The table serves to show the great scatter in the contrail RF estimates but it omits to say
- that the Marquart et al and the Frömming et al estimates are for line-shaped contrails only whereas the other estimates are for contrail cirrus.
- the main difference between the contrail cirrus modeling studies are the different ways of treating contrails,

keeping them separate from natural clouds or treating them with the cloud scheme, and the contrail initialization. The Chen and Gettelman study follows a very different approach from the others.
- That there is another estimate for contrail cirrus RF (Bock and Burkhardt, 2016 – which is already in the literature list) that lies in between the Schumann et al. and the Burkhardt and Kärcher estimate. This means that 3 of 4 estimates lie close together.
- Chen and Gettelman include contrail-contrail overlap since overlap is dealt with in the cloud scheme. The model assumes maximum random overlap for clouds. Only at the initialization stage contrails (age of up to ~30 min.) do not overlap but that is not the same as no overlap between contrails in general. That means that the scatter between contrail cirrus RF estimates is much smaller than suggested by the current table 1 and that the scatter is not due to the overlap scheme. Even though the uncertainty in the overlap between clouds and contrails leads to an uncertainty in contrail cirrus RF, the results from the literature do not demonstrate this fact as they tend to use the same overlap scheme. The range of net RF due to contrail cirrus encompasses the estimate of this study only because estimates for line-shaped contrails are included here.
A deep analysis of previous literature has been done for this revision. Table 1 has been completely rebuilt, adding two new parts (now Tables 2 and 3), and each part reviewed for accuracy. Additionally, a whole section (Section 2) has been added to better address existing literature. This new section in particular benefited greatly from the comments of both reviewers and Michael Ponater, for which we are grateful. We no longer list the Chen and Gettelman (2013) estimate in Table 2, and instead discuss their approach on contrail-contrail overlaps on lines 185-188 of Section 2.2.

2. Biofuels have little impact on contrail formation likelihood but instead on soot number emissions, ice nucleation and contrail life times and optical depth (Moore et al. 2017, Kärcher et al. 2018, Burkhardt et al. 2018)
We have adjusted this comment to make clearer that biofuels will affect the properties of contrails, and not necessarily their likelihood of formation (line 67).

3. Marquart et al (2003) and Frömming et al. (2011) both use the contrail parameterization of Ponater et al. (2002) and simulate line-shaped contrails of varying optical depth including those with an optical depth smaller than 0.02. They both calculate the fractional increase in cloudiness due to contrails. Only the overlap was calculated differently.
This has been corrected in Table 1.

4. Chen and Gettelman do not assume zero overlap between linear contrails when calculating radiation. Instead they use the overlap scheme of CAM (maximum random) in order to take care of overlap between different clouds.
This has been corrected in Table 3. Since Chen and Gettelman (2013) use a very different approach, we no longer list their estimate in Table 2, although it remains in the discussion (lines 185-188).

5. Page 6: You cite papers that determine if cloud-contrail overlap reduces or enhances contrail RF and conclude that this is a major uncertainty instead of mentioning the known fact that the effect depends on the contrail and cloud properties and temperature/height.
We agree that the prior phrasing was incorrect, and that this is a specific issue given that quantifying this dependence is a goal of our paper. We have rephrased the corresponding text in Section 2.1 (lines 169-174). We have also emphasized this in the Introduction in an attempt to better clarify the goals of the paper with regards to investigating this dependence (lines 73-84).

6. On page 7 you talk about contrail-contrail interaction. Please note that interaction can happen due to a number of processes and does not necessarily have to do with radiation.
We have removed this comment as part of the restructuring of Section 1 into two sections.

7. On page 11 the error of the model compared to FL96 is determined. In that context the systematic bias, the underestimation of the dependency on the zenith angle, should be discussed and its impact on the results of this paper.
We agree that this is important. We have extended the discussion in Section 4.1 to draw attention to the possibility of biases combining (lines 721-733). We have also extended the limitations section (Section 5.1) to discuss how these two sources of bias may affect our results (lines 951-954).

8. Line 341-344: All 3 sentences are unclear. It is not clear what it means to aggregate single contrails into one layer! Are coverages due to single contrails added up or not? 'Overlap between . . . is therefore not explicitly resolved': What does that mean – minimum overlap? 'the same approach . . ... as if clouds were centered in the grid cell'. What does that have to do with overlap. Equations would make this text easier to understand.

We have completely rephrased this paragraph, and split it into two for clarity. The comment regarding some overlap not being "explicitly resolved" regarded cases where contrails might form in very close spatial and temporal proximity, an inherent limitation of the version of CERM used here.

9. Line 349: what does '(linear in most cases)' refer to?
This clause has been deleted as it does not add meaning.

10. Line 349: I assume you mean to say that contrail area 'overlaps' and not 'interacts'
Thank you, this has been corrected.

11. Line 353: what is 'potential maximum overlap'
This sentence has been changed to make the intended meaning clearer - that there may be more colinear contrail overlap in flight corriders, while overlaps over areas such as the mainland US may more often inolve unaligned contrails (lines 419-430).

12. Line 355-357: even more useful would be a higher temporal and vertical resolution. The lower the resolution the larger the overlap.
We agree. We have extended our discussion of the advantages of greater temporal and vertical resolution (lines 989-995).

13. In order to correct for errors in the model the authors use for the clear-sky estimates CERES data. Without any discussion where the errors are coming from it is difficult to understand if this approach is acceptable. The radiation emitted from the cloud could still be affected by this error which would mean that the estimated contrail RF would include this model error.
Lolli et al. (2017) found that the regression used by Corti and Peter (2009) to estimate longwave emissivity resulted in significant errors for lack-body temperatures greater than 288 K. We assume that those temperatures are most relevant to the surface, for which we now use the clear-sky CERES estimate. We have added clarifying sentences to this effect on lines 289-306.

14. The term 'independent overlap' needs to be defined.
In this work we distinguish between 'independent contrails' and 'overlapping contrails' with regards to how RF is calculated. This has been clarified in the caption for Table 4 (line 922). We compare 'independent' contrails to 'overlapping' contrails, with the former treating contrails as if there was no radiative interaction between them. A comparison between both cases can also be found in Section 4.1.1.

15. Line 434: The asymmetry parameter in Schumann et al is 0.787 (and not 0.77) for older contrails and 0.827 for younger contrails.
The choice of 0.77 is based on an analysis in a recent paper (Sanz-Morère et al 2020) which drew on the results from Schumann et al (2017) among others. We have extended the reference list appropriately and have added a brief explanation of how the number 0.77 was determined (lines 518-521).

16. Line 503: Figure 3b is the upper right panel
This has been corrected.

17. Line 854: You probably meant to cite Kärcher et al., 2009 and not 2002.
This has been corrected.

18. Line 886 – 888: Those conclusions depend very much on the type of clouds you prescribed. In the tropics many very thick clouds can be found and differences between cloud and contrail top temperature can be very large as well.
This is true. A comment to this effect has been added in the conclusions (line 1044).

Specific comments from Michael Ponater

Introductory remarks

I find this work of Sanz-Morere et al. quite interesting as it emphasizes an important aspect in contrail radiative impact studies that usually has not been investigated as systematically as is done here. In this respect, I feel the two official referees have taken a somewhat stern attitude towards the paper. I think that using a parameter scanning approach in assessing cloud-contrail and contrail-contrail overlap situations goes beyond what currently available studies have done. Figure 3 of the present paper is certainly worthwhile providing. Yet, the referees are certainly right when reminding the authors not to overreach their conclusions, given the limitations of the model framework used in the paper. It is also true, I agree, that some aspects (and even whole papers) of previous research work has been overlooked by the authors.
However, this specific comment is mainly written to provide additional information (including insider knowledge of previous papers) that can help to rectify some statements where the authors – in my view - have interpreted previous work inaccurately.

We would like to express our gratitude to Dr. Ponater for taking the time to read and comment on our manuscript. Based on this comment, and those of the reviewers, we have dramatically reworked our introductory section (now two sections), including an extended discussion of previous work which was previously not well represented.

General comments

- *Contrail-cloud overlap has been generally accounted for in previous contrail radiative impact studies in the way the contrail radiative forcing is usually given under clear-sky as well as all-sky conditions (Myhre and Stordal, 2001; Stuber and Forster, 2007; Yi et al., 2012, and others cited by the authors). It has been a common finding that both the shortwave and the longwave radiative forcing decrease in magnitude under cloudy-sky conditions. Often, but not always, the daily mean net radiative forcing gets more positive with natural clouds included.*

We now dedicate a subsection (2.1) to better exploring how previous studies have quantified cloud-contrail overlap. We hope that this section provides a fairer evaluation of the literature, and better highlights the contribution of our work.

- *As rightly pointed out by referee 2, contrail-contrail overlap has usually been accounted for in contrail studies with global climate models (Marquart et al., 2003; Rap et al., 2010, Burkhardt and Kärcher, 2011; Bock and Burkhardt, 2016), except for when used in idealized setups like the GCMs (ECHAM and CNRM) contributing to Myhre et al. (2009). For illustration what situations can occur in climate models, I reproduce a figure from the PhD thesis of Marquart (2003, unfortunately only available in German language). This picture makes it clear that layers with contrails not only may overlap with layers containing natural cloud, but that situations with contrails and natural clouds existing side by side in the same grid box are also possible. That renders the overlap situations in models like that rather complicated, even if the overlap principle is straightforward. Anyway, it is clear that the climate model parameterizations can include the effect. Possible grid box column situations containing contrails (yellow) and natural clouds (grey) in the ECHAM4 model of Ponater et al. (2002), Marquart (2003), and Marquart et al. (2003). Adapted from Marquart, 2003, her Figure 2.7.*

Thank you very much for this insightful comment and for the useful illustration. We agree and acknowledge that our approach is an approximation only, and is most useful for quantifying an upper bound of multiple layers overlaps impacts on contrail attributable net RF. We have modified our literature review to more accurately reflect the approach taken in GCMs (Section 2), with references added in Tables 2 and 3.

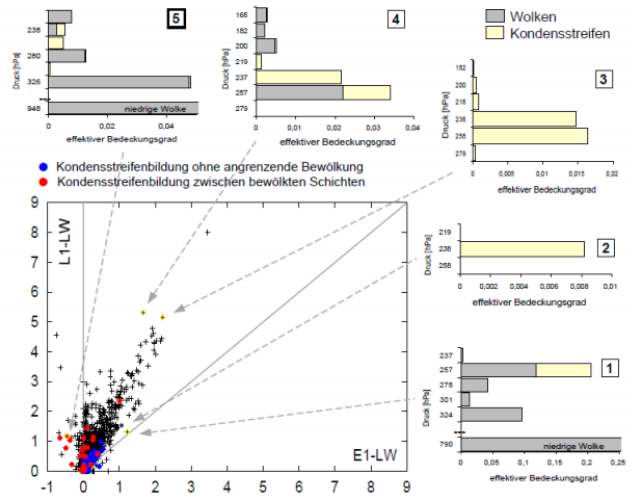

Possible grid box column situations containing contrails (yellow) and natural clouds (grey) in the ECHAM4 model of Ponater et al. (2002), Marquart (2003), and Marquart et al. (2003). Adapted from Marquart, 2003, her Figure 2.7.

Specific comments

- *It is important to realize that the GCM studies (at least those based on the ECHAM climate model) use the maximum-random overlap scheme for calculating radiative fluxes in all sky columns. This refers to contrail-cloud overlap as well as to contrail-contrail overlap situations. See, for example, Figure 4 in Marquart and Mayer (2002).*

This has been added in Table 2 as well as in section 2.1.

- *It may be of interest for the present study that the use of the maximum-random overlap principle has been shown to create severe problems when used in an unfavorable parameterization combination, as discussed by Marquart and Mayer (2002). This has caused the radiative forcing values given by Ponater et al. (2002) to be basically incorrect (amended in Marquart et al., 2003).*

We agree that this caveat is important. We have reviewed Marquart et al (2003), Marquart and Mayer (2002), and Ponater et al (2002), and have attempted to synthesize this in Section 2.1 (lines 135-140).

- *It is not correct (as given in your Table 1) that the overlap assumption in the studies of Marquart et al. (2003) and Frömming et al. (2011) is different. Both use the maximum-random overlap principle in the radiative transfer calculations, as do Burkhardt and Kärcher (2011).*

We have re-reviewed the appropriate literature and corrected our summary accordingly. This is now reflected in Table 2.

- *Note that the ECHAM4 studies of Ponater et al. (2002), Marquart et al. (2003), and Frömming et al. (2011) mainly give mean optical depth values of visible contrails (i.e., averaged over those contrails that exceed a "visibility threshold" of 0.02), to enable comparison with observations. However, the "invisible"contrails are not excluded from the radiative forcing calculations. This may confuse an unaware viewer of your Table 1. I also note that the visibility threshold has been a subject of debate. According to Kärcher et al. (2009) a threshold value of 0.05 is more appropriate and has been preferred in later studies (e.g., Bock and Burkhardt, 2016).*

We have updated Table 1 accordingly, and attempted to added a brief discussion in Section 3.2.4 regarding assumptions on satellite contrail visibility, and how "invisible" contrails are treated in radiative forcing calculations (lines 447-474).

- *The global mean optical depth value of 0.05 given in Table 1 for the Frömming et al. (2011) results seems to be incorrect. Table 2 in that paper provides the consistent value of 0.08. The confusion may originate from the first paragraph of Frömming et al.'s section 3.1, where the optical depth of all contrails (including "invisible" ones below 0.02) is additionally given, and this one is indeed 0.05.*

Table 1 has been corrected accordingly.

- *Finally I recommend to split your Table 1 into two parts, one referring to lineshaped contrails (first two rows), and one to contrail cirrus (last four rows). Otherwise any reader observing totally different radiative forcings for*

nearly the same air traffic volume will be misleaded and will mistakenly be tempted to attribute the difference to the cloud overlap assumptions!
We agree that this improves the paper significantly. We have split Table 1 as suggested.

- *Line 89: As stated above, I disagree with the claim that Frömming et al. (2011) assume random overlap in the radiative transfer calculations.*

This has been corrected.

- *Line 239: Do you mean sufficiently thick or sufficiently extended? Yet, either assumption appears to be somewhat bold for contrails, I think.*

We have clarified this on line 308. This is a significant assumption, and one which we would like to investigate in more detail in the future. The overall error for contrails has previously been estimated at around 10% (Gounou and Hogan 2007) (line 312), but may be greater for the purposes of investigating contrail overlap specifically. We state this in our Limitations section (lines 937-940) but now also include a statement that the inclusion of 3-D effects would be a productive topic for future work (line 1021).

- *Line 256: "Due to the known strong dependence …" I think at this point the fundamental work of Markowicz and Witek (2010) on the subject ought to be acknowledged.*

This reference has been added on line 326.

- *Line 408: Here, or somewhat earlier, the notion of "quantifying the effect of cloud overlap by the difference of all-sky minus clear-sky" should be scrutinized a little bit. The point is that Rap et al. (2010) extensively discuss the potential effect of a correlation between contrails and natural clouds, increasing the frequency of all-sky situations with respect to clear-sky situations in comparison with a setup assuming climatological background (natural) clouds. My impression is that you do not account for this correlation in your calculation setup. If this is true, it might be fair to mention this as a caveat.*

We now include this in our opening literature review, but given the concerns regarding this work specifically we have also added a discussion on this topic in the Limitations section (lines 962-969).

- *Line 431: I think that there are also many contrails below 0.05 (see Kärcher et al., 2009). This only supports your approach to extend your parameter space down to tau = 0!*

This is a good point – we have corrected line 516 to emphasize this strength.

- *Line 439: In situ measurements like the one cited here may not fully represent the parameter range of contrails, hence you might consider to add some citation of a satellite study such as Bedka et al. (2012) or Minnis et al. (2013).*

We have reviewed the studies suggested to ensure that our parameter range is reasonable, and have added them as references (section 3.1.1).

We would again like to thank the reviewers for their time and insight, and believe that their input during this review process has improved the paper substantially. Thank you again for considering our manuscript for publication in *Atmospheric Chemistry and Physics*, and we look forward to your response.

Best wishes,

Sebastian Eastham

References

Chen, C.-C. and Gettelman, A.: Simulated radiative forcing from contrails and contrail cirrus, Atmos. Chem. Phys., 13(24), 12525–12536, doi:10.5194/acp-13-12525-2013, 2013.

Corti, T. and Peter, T.: A simple model for cloud radiative forcing, Atmos. Chem. Phys., 9(15), 5751–5758, doi:10.5194/acp-9-5751-2009, 2009.

Davis, S. M., Hegglin, M. I., Fujiwara, M., Dragani, R., Harada, Y., Kobayashi, C., Long, C., Manney, G. L., Nash, E. R., Potter, G. L., Tegtmeier, S., Wang, T., Wargan, K., and Wright, J. S.: Assessment of upper tropospheric and stratospheric water vapor and ozone in reanalyses as part of S-RIP, Atmos. Chem. Phys., 17, 12743–12778, https://doi.org/10.5194/acp-17-12743-2017, 2017.

Dessler, A. E. and Yang, P.: The Distribution of Tropical Thin Cirrus Clouds Inferred from Terra MODIS Data, J. Clim., 16(8), 1241–1247, doi:10.1175/1520-0442(2003)16<1241:TDOTTC>2.0.CO;2, 2003.

Jiang, J. H., Su, H., Zhai, C., Wu, L., Minschwaner, K., Molod, A. M., and Tompkins, A. M. (2015), An assessment of upper troposphere and lower stratosphere water vapor in MERRA, MERRA2, and ECMWF reanalyses using Aura MLS observations, *J. Geophys. Res. Atmos.*, 120, 11,468– 11,485, doi:10.1002/2015JD023752.

Kärcher, B., U. Burkhardt, S. Unterstrasser, and P. Minnis (2009), Factors controlling contrail cirrus optical depth, Atmos. Chem. Phys., 9(16), 6229–6254, doi:10.5194/acp-9-6229-2009.

Minnis, P., Duda, D., Palikonda, R., Bedka, S., Boeke, R., Khlopenkov, K., Bedka, K., Chee, T., 2011. Estimating Contrail Climate Effects from Satellite Data, 3rd AIAA Atmospheric Space Environments Conference. https://doi.org/10.2514/6.2011-3375

Simone, N.W., Stettler, M.E.J., Barrett, S.R.H., 2013. Rapid estimation of global civil aviation emissions with uncertainty quantification. Transp. Res. Part D Transp. Environ. 25, 33–41. https://doi.org/10.1016/j.trd.2013.07.001

Schumann, U., Mayer, B., Graf, K. and Mannstein, H.: A Parametric Radiative Forcing Model for Contrail Cirrus, J. Appl. Meteorol. Climatol., 51(7), 1391–1406, doi:10.1175/JAMC-D-11-0242.1, 2012.

Effect of contrail overlap on radiative impact attributable to aviation contrails

Inés Sanz-Morère[1], Sebastian D. Eastham[1], Florian Allroggen[1], Raymond L. Speth[1], Steven R. H. Barrett[1]

[1]Laboratory for Aviation and the Environment, Massachusetts Institute of Technology, Cambridge, MA 02139, United States of America

Corresponding author: Sebastian Eastham (seastham@mit.edu)

Abstract. Condensation trails ("contrails") which form behind aircraft are estimated to cause on the order of 50% of the total climate forcing of aviation, matching the total impact of all accumulated aviation-attributable CO_2. The climate impacts of these contrails are highly uncertain, in part due to the effect of overlap between contrails and other cloud layers. Although literature estimates suggest that overlap could change even the sign contrail radiative forcing, the impacts of cloud-contrail overlaps are not well understood, and the effect of contrail-contrail overlap has never been quantified. In this study we develop and apply a new model of contrail radiative forcing which explicitly accounts for overlap between cloud layers. Assuming maximum possible overlap to provide an upper bound on impacts, cloud-contrail overlap is found to reduce the shortwave cooling effect attributable to aviation by 66%, while reducing the longwave warming effect by only 37%. Therefore, on average in 2015, cloud-contrail overlap increased the net radiative forcing attributable to contrails. We also find sensitivity of contrail radiative forcing to cloud cover with respect to geographic location. Clouds significantly increase warming at high latitudes and over sea, transforming cooling contrails into warming ones in the North-Atlantic corridor. Based on the same data, our results indicate that disregarding overlap between a given pair of contrail layers can result in longwave and shortwave radiative forcing being overestimated by up to 16% and 25% respectively, with the highest bias observed at high optical depths (> 0.4) and high solar zenith angles (>

75°). When applied to estimated global contrail coverage data for 2015, contrail-contrail overlap reduces both the longwave and shortwave forcing by ~2% relative to calculations which ignore overlap. The effect is greater for longwave radiation, resulting in a 3% net reduction in the estimated RF when overlap is correctly accounted for. This suggests that contrail-contrail overlap effects can likely be neglected in estimates of the current-day environmental impacts of aviation. However, the effect of contrail-contrail overlap may increase in the future as the airline industry grows into new regions.

1 Introduction

Condensation trails ("contrails") are ice clouds which form in aircraft engine exhaust plumes. Contrails cause "cooling" effects, by scattering incoming shortwave solar radiation (RF_{SW}), as well as "warming" effects, by absorbing and re-emitting outgoing terrestrial radiation (RF_{LW}). Previous studies have found the latter effect to be dominant, particularly at night when the cooling effects associated with reductions in incoming shortwave radiation do not exist (Liou, 1986; Meerkötter et al., 1999). The difference between these two effects is the contrail-attributable radiative forcing (RF) (Penner et al., 1999; IPCC 2013).

Table 1. Existing estimates of the longwave (LW), shortwave (SW), and net radiative forcing (RF) attributable to contrails. ([1]: Estimated fuel burn for 2000 and 2002 taken from Olsen et al., 2013; [2]: From Ponater et al., 2002, which reports on the same data; *: definition of "visible" varies between studies, and is clarified in the main text)

Source	Target element	Target year	Fuel burn [Tg]	Global mean optical depth ($\bar{\tau}$)	RF_{LW} [mW/m^2]	RF_{SW} [mW/m^2]	Net RF [mW/m^2]	Contrail modeling
Marquart et al., 2003	Linear/visible* contrails (or lifetime < 5h)	1992	112.0	0.15[2]	+4.9	-1.4	+3.5	Fractional coverage in ECHAM4
Frömming et al., 2011		2000	152.0[1]	0.08	+7.9	-2.0	+5.9	
Burkhardt and Karcher, 2011		2006	151.6	/	+5.5	-1.2	+4.3	CCMod in ECHAM4
Spangenberg et al., 2013		2006	151.6	/	+9.6	-3.9	+5.7	Coverage from Aqua MODIS
Burkhardt & Kärcher, 2011	Contrail cirrus	2002	154.0[1]	0.05	+47	-9.6	+38	CCMod in ECHAM4
Chen & Gettelman, 2013		2006	151.6	/	+41	-26	+15	Fractional volume in CAM5
Schumann et al., 2013		2006	151.6	~0.2	+126	-77	+49	Lagrangian contrail model (CoCiP)
Schumann et al., 2015		2006	151.6	0.34	+143	-80	+63	
Bock and Burkhardt, 2016a		2006	151.6	/	/	/	+56	CCMod in ECHAM5

The net radiative forcing impacts of contrails have been quantified using both global climate models (GCMs) (e.g. Chen and Gettelman, 2013; Ponater et al., 2002) and dedicated modeling approaches such as the Contrail Cirrus Prediction Tool (CoCiP) (Schumann, 2012) and the Contrail Evolution and Radiation Model (CERM) (Caiazzo et al., 2017). These approaches have resulted in estimates of total contrail radiative forcing ranging from +15.2 mW/m^2 (Chen and Gettelman, 2013) to +63.0 mW/m^2 (Schumann et al., 2015) for 2006, as shown in Table 1. Normalizing by the total aviation fuel burn in each given year, this gives a range of +0.1 to +0.4 $mW/m^2/Tg$. As such, the net radiative forcing impacts of contrails are comparable in magnitude to the radiative forcing impacts of aviation-attributable CO_2 emissions, which Lee et al. (2009) estimated at +0.12 $mW/m^2/Tg$.

The scaling of contrail radiative forcing impacts with future traffic growth will depend on multiple factors, especially (i) potential changes in contrail properties with changes in engine efficiency and the use of biofuels (Schumann, 2000; Caiazzo et al., 2017; Kärcher et al., 2018); (ii) the emergence of new markets with different prevailing atmospheric conditions (Boeing, 2019); and (iii) increased likelihood of contrail-contrail overlap as existing markets and flight paths become more saturated. Major uncertainties on contrail radiative forcing estimation are related to the available data on ice supersaturation in the atmosphere, and the growth and lifetime of contrails (Schumann and Heymsfield, 2017, Kärcher, 2018).

The objective of this work is to provide a consistent, quantitative analysis of the effect of overlap between natural and artificial cloud layers (both cloud-contrail and contrail-contrail) on contrail attributable radiative forcing. This includes both parametric analysis of individual columns and an assessment of how global contrail RF is affected. The impact of natural clouds on contrail radiative forcing has been repeatedly identified as an important contributor to overall contrail impacts, but significant uncertainty remains regarding the magnitude of the effect (Markowicz and Witek, 2011a; Schumann et al., 2012; Spangenberg et al., 2013; Schumann and Heymsfield, 2017). Contrail-contrail overlap has been modeled in the past as a component in contrail RF estimates, but no work has yet been published which quantifies its contribution to overall forcing. Furthermore, the response of overlapping impacts to variations on local

conditions, including cloud properties, atmospheric conditions, and surface properties, has not been parametrically quantified. This work aims to provide insight into how each of these factors affects the impact of multiple-layer overlap on contrail attributable radiative forcing.

We start by reviewing existing literature on cloud layer overlap modeling in the context of contrails, including past studies modeling cloud-contrail and contrail-contrail overlaps (Section 2). We then present the radiative forcing model (Section 3.1) and its input data (Section 3.2), followed by the experimental design used to compute the effects and sensitivities of cloud layer overlap (Section 3.3).

We present three analyses. Firstly (Section 4.1), we perform a parametric study to quantify the effect of multiple layer overlap on the RF attributable to a single contrail. This includes the effect of variations in parameters such as optical depth and ambient temperature. Alongside this parametric evaluation, we also evaluate our model results against the widely-used Fu-Liou radiative transfer model. Secondly (Section 4.2), we expand this parametric analysis to quantify how the effect of overlap varies with location and season, using estimated global atmospheric data for 2015. Thirdly (Section 4.3), we estimate the specific contribution of multiple layer overlaps to the simulated 2015 global contrail radiative forcing, isolating both cloud-contrail and contrail-contrail impacts.

These analyses are followed by a discussion of limitations to our approach, and potential avenues for future research (Section 5). This includes limitations associated with the base RF model and with the representation of cloud overlap.

2 Review of past approaches for modeling cloud layers overlaps in contrail-related studies

Past studies have shown that overlapping with other cloud layers is likely to reduce both the shortwave (cooling) and longwave (warming) RF associated with contrails. However, there is little agreement on how cloud-contrail overlap might change the net RF, due to uncertainty over whether they would more strongly mitigate the shortwave or longwave component. Meanwhile contrail-contrail specific impact on

global contrail RF has never been quantified. In this section we discuss previous literature addressing the treatment of multiple layer overlap in the context of contrail radiative forcing calculations.

2.1 Previous examples of cloud-contrail overlap modeling

Table 2. Previous evaluations of the effect that overlap with natural clouds has on contrail RF. MRO: Maximum-Random Overlap; defined by Geleyn and Hollingsworth (1978) as assuming that clouds in adjacent layers are maximally overlapping, while clouds separated by one or more clear layer are randomly overlapping. ECMWF: European Centre for Medium-Range Weather Forecasting. RT: Radiative Transfer. +/-/=: increase/ decrease/ remains the same – impact on net RF from clouds, +/- means that both effects have been found depending on clouds properties. *Only linear contrails considered.

Source	Net effect of overlap on contrail RF	Cloud-contrail overlap modeling
Minnis et al., 1999	+/-	Contrail coverage randomly overlaps with other clouds. Effect varies with type of cloud
Meerkotter et al., 1999	+	Various RT models tested. Only effect of low-level cloud overlap with contrails is evaluated
Myhre and Stordal, 2001	=	ECMWF cloud coverage. Fixed contrail altitude and monthly mean cloud data. Multistream RT model from Stamnes et al., 1988.
Marquart et al., 2003	-	MRO used for each vertical column
Stuber and Forster, 2007	-	Fu-Liou RF model, slight reduction of global contrail RF due to clouds
Radel and Shine, 2008	-	Random overlap, net reduction of approximately 10%
Myhre et al., 2009	-	Intercomparison between RT models. Small reductions
Rap et al., 2010	-	Random overlap, net reduction up to 40% with on-line model
Fromming et al., 2011	-	MRO used for each vertical column
Markowicz and Witek, 2011a	+/-	Net impact varies with assumed crystal shape in contrails
Schumann et al., 2012	+/-	Parametric RF model applicable to CoCiP's contrail data. Clouds modelled as RF reduction function of optical depth.
Yi et al., 2012	-	Sensitivity to overlap assumption. Slight reduction due to natural clouds.
Spangenberg et al., 2013	+/-	Fu-Liou RTM with input data from Aqua MODIS (Minnis et al. 2008). Effect varies with type of cloud.

Studies have used observational data to quantify the effect of natural overlap on contrail RF. Spangenberg et al. (2013) found a reduction in both $|RF_{LW}|$ and $|RF_{SW}|$ from contrails in the presence of natural clouds, with $|RF_{SW}|$ falling by 30% [40%] in the presence of an ice [water] cloud. This resulted in a decrease [increase] in net RF – demonstrating the difficulty of evaluating the impact of natural clouds on the net

contrail RF. Another assessment using a simple model of contrail coverage based on observational data indicated that, while low-level marine clouds could significantly increase contrail net RF, cirrus clouds could have the opposite impact by more significantly reducing RF_{LW} than RF_{SW} (Minnis et al., 1999).

Single-column analyses have also been performed. An estimate using fixed global contrail coverage for a single month from Myhre and Stordal (2001) found that the net impact of cloud overlap on contrail RF is close to zero, as the effect on RF_{LW} and RF_{SW} was similar. They performed no specific evaluation of the dependence on local conditions and cloud properties. Another study by Myhre et al. (2009), comparing multiple radiative transfer models, found a consistent reduction in contrail RF due to natural clouds, with a maximum decrease of 14%. Meerkötter et al. (1999) also compared radiative transfer models, including the effect of crystal shape and optical depth. They found that the presence of low level clouds increases the net radiative forcing due to contrails.

A parameterization for line–shaped contrails in a general circulation model (GCM) was presented by Ponater et al. (2002) for ECHAM4 (version 4 European Center/Hamburg General Circulation Model). A later amendment suggested that the assumption of maximum random overlap can cause RF_{LW} to be underestimated by 70% when using certain radiative transfer parameterizations (Marquart et al 2003, Marquart and Mayer, 2002). This indicates the extent of the sensitivity of contrail RF to the assumed overlap scheme.

Marquart et al. (2003), again using ECHAM4, estimated a 10% reduction in linear contrail RF due to the presence of natural clouds. Frömming et al. (2011), using the same model, found the largest radiative impact to occur over regions with few natural clouds. Stuber and Forster (2007) similarly found a 7% reduction in contrail RF due to cloud overlap when accounting for diurnal variations in air traffic.

Both Radel and Shine (2008) and Rap et al (2010) found a reduction in global net RF of approximately 10%, with both $|RF_{LW}|$ and $|RF_{SW}|$ reduced by up to 40% due to cloud masking effects. Rap et al. (2010), adapting Ponater et al.'s (2002) contrail parameterization scheme to the UK Met Office climate model,

also found a correlation between contrail and natural clouds, showing the importance of using accurate (and consistent) natural cloud cover data. Markowicz and Witek (2011a) extended these results by evaluating the role of crystal structure. While still finding a mean net impact on global contrail RF of less than 10%, they also found that this impact changes sign depending on the assumed contrail crystal habit.

CAM5 (Community Atmospheric Model version 5) has also been used to estimate global contrail RF (Yi et al., 2012; Chen and Gettelman, 2013). In Yi et al. (2012) they assess the sensitivity to the assumed form of overlap. Global contrail net RF varies is reduced by 15% when switching the cloud-contrail overlap assumption from random to maximum random (Geleyn and Hollingsworth, 1978). This shows that the choice of overlap scheme can significantly modify the estimated global RF.

Lagrangian models have also been used to simulate contrails, including CoCiP (Schumann, 2012) and CERM (Caiazzo et al., 2017). Schumann (2012) developed an approach to simulate the RF associated with a single contrail, including the impact of natural clouds on contrail RF. They concluded that net RF may increase if contrails overlap with low-level clouds, but that the sign of a contrail's RF could change signs if passing underneath natural cirrus clouds. This again demonstrates the need to accurately model natural clouds when simulating contrails. However, simulations of single contrails cannot easily account for multiple-contrail radiative interactions.

These approaches and their results are summarized in Table 2. The disagreement in these estimates is in large part due to the nature of competing longwave and shortwave components, but also due to uncertainty regarding the role that specific cloud properties and parameters might have in changing the effect of overlap on contrail RF. We here aim to provide additional insight into these relationships through a parametric analysis, extending from a single column up to the global-scale effects of cloud-contrail overlap on contrail RF.

2.2 Previous examples of contrail-contrail overlap modeling

Table 3. Existing methods for modeling contrail-contrail overlap when estimating global contrail RF. MRO: Maximum-Random Overlap, defined by Geleyn and Hollingsworth (1978) as assuming that clouds in adjacent layers maximally overlap while clouds separated by one or more clear layer randomly overlap. *Only linear contrails considered)

Source	Model used to represent contrail-contrail overlap
Minnis et al., 1999	No overlap considered (fractional coverage from observations)
Marquart et al., 2003	MRO in the vertical for each column
Radel and Shine, 2008	Random overlap
Rap et al., 2010	Random overlap
Fromming et al., 2011	MRO in the vertical for each column
Burkhardt and Kärcher, 2011	MRO in the vertical for each column
Chen and Gettelman, 2013	Zero contrail-contrail overlap in grid box
Schumann et al., 2013	Linear RF addition
Bock and Burkhardt, 2016	MRO in the vertical for each column

When contrails are simulated in global climate models, contrails (and contrail overlaps) are treated in several different ways (see Table 3). A contrail parametrization has been developed for ECHAM4 (Ponater et al., 2002) in which maximum random overlap is assumed between contrail and cloud layers (Marquart et al., 2003; Fromming et al., 2011; Burkhardt and Kärcher, 2011; Bock and Burkhardt, 2016). Radel and Shine (2008) and Rap et al. (2010) also employ this parameterization, calibrating the results using satellite observations. Chen and Gettelman (2013) also implemented contrails in the CAM5 model, representing them as an increase in the 3-D cloud fraction. However, they assumed zero overlap between linear contrails if located in same vertical level (~1 km). Finally, the CoCiP Lagrangian contrail model (Schumann et al. 2012) indirectly models contrail-contrail overlaps by linearly summing the RF of all contrails while accounting for any cirrus which was observed above the simulated contrail. However, this does not explicitly account for interaction between simulated contrails.

Differences can be observed in the way contrail-contrail overlaps are modeled in literature. While the optimal approach is not clear, no study to date has quantified the effect of contrail-contrail overlap on global contrail RF. Assuming continued growth in the aviation industry, more instances of contrail

overlap can be expected to occur. Better understanding of the magnitude and behavior of contrail-contrail overlap is therefore needed. In this work, we aim to provide insight into the factors which affect the sign and magnitude of changes in contrail RF due to contrail-contrail overlap. We also provide a first quantification of the current-day magnitude of its effect on global contrail RF.

3 Method

The modeling approach is based on a radiative transfer model previously developed to simulate natural clouds, which we extend to simulate multiple contrail cloud layers. Section 3.1 describes the model and validates the results against existing approaches, and Section 3.2 describes the input data. Using this model, we develop a series of simulations - described in Section 3.3 - which quantify the net radiative forcing impacts of contrail-contrail overlaps and cloud-contrail overlaps under different conditions.

3.1 The radiative forcing model

The net radiative forcing (RF) attributable to contrails is the sum of two components: longwave (LW) and shortwave (SW). Shortwave radiation is the incoming radiation flux from the sun, which typically undergoes scattering and reflection with minimal atmospheric absorption or re-emission. Longwave ("terrestrial") radiation is the emission of longer-wavelength infrared radiation by the Earth, which undergoes minimal scattering or reflection but is strongly absorbed by clouds before being re-emitted. Contrail cloud layers induce a negative shortwave RF during the day since they reflect incoming solar radiation, slightly increasing the global mean albedo. However, as in the case of natural cirrus clouds, the longwave RF impacts of contrails during both day and night are positive. This is because they absorb terrestrial radiation and re-emit it at the lower temperatures of the upper troposphere (Penner et al., 1999).

In this study we extend and use a cloud radiative transfer model first described by Corti and Peter (2009) which can be applied to both natural or artificial cloud layers (e.g. contrails). This model calculates the cloud-induced change in outgoing longwave and shortwave radiation based on simulated or observed surface conditions (albedo and surface temperature), outgoing longwave flux, meteorological data (ambient temperature), and cloud coverage. The radiative forcing (RF) attributable to a single cloud layer

is calculated using two simulations: one with the cloud layer present, and one without. The instantaneous RF of a cloud layer is then defined as the difference between the net radiative flux at the top of the atmosphere with and without the layer (IPCC, 2013), so a positive net radiative forcing impact implies an increase in the net energy of the Earth-atmosphere system.

3.1.1 Summary of the single cloud layer RF model

The radiative forcing model quantifies the instantaneous RF per unit area of cloud layer. A full description is given in the original model description paper (Corti and Peter, 2009), but we give a brief summary here.

In the original model, the longwave RF is calculated in W/m^2 for a single cloud layer as

$$\boldsymbol{RF_{LW} = L - L_c = \varepsilon\sigma^*(T_{srf}{}^{k*} - T_c{}^{k*})} \quad (1)$$

where L is the outgoing longwave radiation from the surface of the Earth (in W/m^2); L_c is the total outgoing longwave radiation from the cloud (in W/m^2); T_{srf} is the temperature of the Earth's surface (in K); T_c is the cloud temperature (in K); ε is the contrail emissivity; and σ* (the adjusted Stefan-Boltzmann constant, in W/m^2/K$^{-2.528}$) and k^* (= 2.528) are constants (Corti and Peter, 2009). Therefore $\varepsilon\sigma^* T_c{}^{k*}$ represents the longwave radiation emitted by the cloud (in W/m^2) accounting for CO_2 and water vapor absorption from the atmosphere (Corti and Peter, 2009). The double-counting of atmospheric absorption is inherent to the original model. More information can be found in Section 5.1. Additionally, due to limitations of this approach identified by Lolli et al. (2017), we use an alternative approach for estimating the outgoing longwave flux at the Earth's surface (Section 3.1.2).

The shortwave RF is calculated as

$$\boldsymbol{RF_{SW} = -S \cdot t \cdot (1 - \alpha)\left(\frac{R_c - \alpha R_c'}{1 - \alpha R_c'}\right)} \quad (2)$$

where S is the incident solar radiation (in W/m^2); R_c is the cloud reflectance for direct radiation; R_c' is the cloud reflectance for diffuse radiation; α is the albedo of the Earth; and t is the atmospheric transmittance above the cloud, assumed constant at a value of 0.73 (Corti and Peter, 2009). The adjusted constants (σ^* and k^*) and daily mean atmospheric transmittance (t) are based on clear sky simulations combining results from a high-fidelity radiative transfer model and ECMWF ERA-40 atmospheric profiles (Fu and Liou, 1993; Corti and Peter, 2009). Assuming a constant transmittance may result in some bias, as the parameter t would likely vary with location, time and atmospheric composition, including column concentrations of water vapor and aerosols (Schwarz et al. 2020).

While most of the parameters previously mentioned describe the atmospheric conditions, three parameters describe the interaction between clouds and radiation: longwave emissivity (ε) and shortwave reflectances (R_c and R_c'). All three are dependent on the layer optical depth τ. Shortwave reflectances, representing cloud interaction with sunlight, are additionally dependent on cloud layer microphysics through the asymmetry parameter g and R_c' is additionally dependent on the solar zenith angle. A full description of this derivation is given in Corti and Peter (2009).

The optical properties of contrail ice crystals are represented in the model by the asymmetry parameter g of the layer. g measures the degree of anisotropy of scattering and is dependent on the radius and shape of the particle mixture. It ranges from -1 (total backscatter) to +1 (total forward scatter), while equaling 0 for perfect isotropic scattering (Stephens et al., 1990). Ice cloud particles have complex scattering phase functions (Liou et al., 1998; Baran, 2012) but typically fall into the Mie scattering regime with a dominant forward scattering peak, corresponding to an asymmetry parameter between 0.7 and 0.9 (Baran, 2012; Nousiainen and McFarquhar, 2004; Yang et al., 2003). The effect of uncertainty in the asymmetry parameter on contrail RF is investigated in a complementary study (Sanz-Morère et al., 2020). We here assume an average contrail asymmetry parameter, based on in situ measurements, of 0.77 with an increase for the first hour to account for short-term changes in crystal shape (g = 0.78) (Febvre et al., 2009; Gayet et al., 2012; Bedka et al., 2013; Minnis et al., 2013; Schumann et al., 2017; Sanz-Morère et al., 2020). For natural clouds, the asymmetry parameter is calculated as a function of altitude only. We assume that

clouds below 8 km have an asymmetry parameter of 0.85 (typical of liquid water clouds); that clouds above 10 km have an asymmetry parameter of 0.7 (typical of long-loved cold cirrus clouds); and that clouds between 8 and 9 km have an asymmetry parameter of 0.8 (Gerber, 2000; Jourdan, 2003; Kokhanovsky, 2004; Schumann et al., 2017)

3.1.2. Modification, limitations, and validation of the radiative transfer model

We have modified the original approach described by Corti and Peter to account for limitations highlighted by Lolli et al. (2017). Firstly, the original model estimates outgoing longwave flux at the surface by applying a fixed relationship between surface temperature and emitted radiation, based on data from the ECMWF ERA-40 meteorological product. Lolli et al. (2017) found that, below surface temperatures of 288 K, this yielded results that agreed (within 6%) with those from the more complex Fu-Liou-Gu radiative transfer model (Liou, 1986; Fu et al., 1997). However, they also found that for surface temperatures greater than 288 K, this approach is inaccurate and results in radiative forcing errors of approximately 65%. They identified that the source of this error was the regression used by Corti and Peter (2009) to estimate longwave emissivity in the context of high surface temperatures.

To overcome this issue, we instead use a "top-down" approach in which radiative forcing (longwave) is calculated as the difference between the estimated top-of-atmosphere longwave flux under "clear sky" conditions (without clouds), and the longwave flux perturbed by cloud layer(s). This removes the need to use the regression from Corti and Peter (2009) when calculating surface emissivity, which is the most likely context in which such high temperatures will be encountered. The estimated outgoing longwave radiation in the absence of clouds (OLR_{clear}) is provided in the CERES data product (see Section 3.2.3). This value of outgoing longwave radiation is estimated to have an error of approximately 1.7% (Loeb et al., 2018). However, we do not propagate this error further through our calculations. Hence, we calculate longwave radiative forcing due to contrails as

$$\boldsymbol{RF_{LW} = \varepsilon OLR_{clear} - L_c = \varepsilon OLR_{clear} - \varepsilon\sigma^{*}T_c^{k*}} \quad (3)$$

with all other terms as described in Equation (1).

Shortwave radiative forcing is calculated by assuming a constant atmospheric transmittance above the cloud layer, which may result in inaccuracy when considering clouds at different altitudes. This constant value is calculated based on average estimates from a high-fidelity radiative transfer model (Fu and Liou, 1993). Lolli et al. (2017) found that the error due to this assumption was negligible, and so we retain it in our model.

We also assume that cloud layers are of sufficient horizontal extent that 3-D effects (due to horizontal propagation of radiation) are negligible. The effect of this assumption has been investigated in detail previously (Gounou and Hogan, 2007; Davis and Marshak, 2010; Barker et al., 2012; Hogan and Shonk, 2013). Due to the low thickness of contrails, the resulting error in RF_{SW} and RF_{LW} is expected to be on the order of 10% (Gounou and Hogan, 2007).

To ensure that our conclusions are realistic, we also validate the model through comparison to two existing radiative transfer model developed for cirrus clouds: the "Fu-Liou" model (hereafter FL96) (Liou, 1986; Fu and Liou, 1993; Fu, 1996) and CoCiP (Schumann et al., 2012). We calculate the radiative forcing due to an isolated contrail layer while varying multiple parameters: contrail optical depth, surface albedo, and solar zenith angle (with fixed radiation data). A full description and evaluation is given in Appendix A. Each of the three models uses a different approach to represent the optical properties of the ice crystals, so initial comparisons are performed by comparing the results when sweeping over a range of input parameters. We find that, for the radiative forcing due to a single contrail, our results match those from CoCiP, with differences of less than 10% for both RF_{LW} and RF_{SW}. Qualitatively, for the same range of particle sizes, FL96 shows similar behavior. However, the magnitude of the calculated radiative forcing differs between our model and FL96, with inconsistencies of up to 40% in RF_{SW}.

Due to the strong dependence of RF_{SW} on crystal size and shape (Markowicz and Witek, 2011b; Sanz-Morère et al., 2020), and due to the different treatment of these properties in the three models tested, we

conduct a deeper analysis on the resulting difference on RF_{SW}. We choose a specific crystal size in FL96 and compare the simulated RF against results from our model using an "equivalent" asymmetry parameter (more information can be found in Appendix A). For a given surface albedo, we find differences of less than 15% at low solar zenith angles, increasing up to 20% at solar zenith angles greater than 80°. This is consistent with prior evaluations of the two-stream approximation used in our model (Coakley and Chylek, 1975; Corti and Peter, 2009), which has reduced accuracy at high solar zenith angles (see Section 5.1). The dependence of RF_{SW} on albedo is also evaluated in each model. Qualitatively the three models show the same behavior with changing albedo, optical depth and solar zenith angle. For albedos below 0.3 the models agree to within 10%, and for albedos below 0.5 the maximum difference is less than 30%. The percentage difference is insensitive to optical depth (see Fig. A2).

3.1.3 Extension to multiple layers

To quantify the effect of cloud-contrail or contrail-contrail overlaps, we extend the model to account for multiple overlapping layers. Computation of longwave RF is accomplished by working outwards from the Earth's surface, as shown in Fig. 1, with each layer absorbing some fraction ε_i of the incident longwave radiation while re-emitting a total flux of $\varepsilon_i \sigma^* T_i^{k*}$. This approach assumes each cloud layer to be at the temperature of the surrounding atmosphere, so that temperature feedbacks can be disregarded and longwave radiation absorption and re-emission is derived from local temperature and surface temperature. Downward fluxes are not shown because the approach neglects temperature feedbacks. As a result, only outgoing radiation is used in our RF calculations. Based on the approach followed in Schumann et al. (2012), we assume RF_{LW} to be always nonnegative, setting the longwave radiative forcing of a contrail to be zero when its temperature is higher than lower layers.

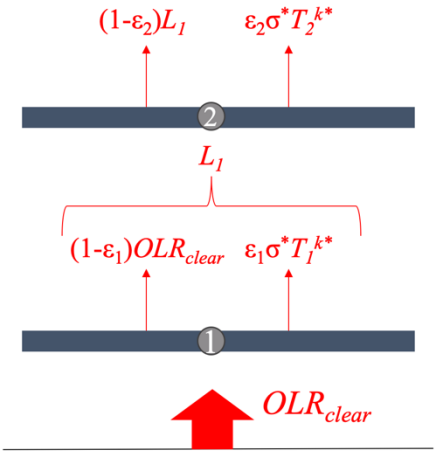

Figure 1. Schematic of longwave RF calculation in a two-layer overlap. Arrows represent emitted or transmitted longwave radiation. L is longwave emission from the Earth's surface, while L_i is the longwave emission from layer i. $\boldsymbol{\varepsilon_i}$ and $\boldsymbol{T_i}$ are emissivity and temperature of each of the layers.

To calculate the shortwave RF, we start by estimating the shortwave radiation impact of each cloud layer. Per unit of direct incident shortwave radiation, a fraction R_c of shortwave radiation is reflected and (1 - R_c) is transmitted (absorption of shortwave radiation is assumed to be negligible). The same approach is taken for diffuse shortwave radiation, this time using the parameter R_c'. The parameters R_c and R_c' are calculated as

$$\boldsymbol{R_c} = \frac{\boldsymbol{\tau/\mu}}{\boldsymbol{\gamma + \tau/\mu}} \quad (4)$$

$$\boldsymbol{R_c'} = \frac{\boldsymbol{2\tau}}{\boldsymbol{\gamma + 2\tau}} \quad (5)$$

where τ is the optical depth of the cloud layer, μ the cosine of the solar zenith angle θ, and γ = 1/(1-g) where g is the layer asymmetry parameter.

Due to the high degree of forward scattering of clouds and contrails (Baran, 2012; Nousiainen and McFarquhar, 2004; Yang et al., 2003; Kokhanovsky, 2004), we further assume that (i) shortwave radiation, which has not yet impinged on the Earth's surface, is direct; and (ii) any shortwave radiation reflected from the Earth's surface is diffuse (Corti and Peter, 2009). With these assumptions, the total

radiative forcing of two overlapping layers with identical asymmetry parameters is analytically equal to the radiative forcing of a single layer with an optical depth equal to the sum of that from both layers. A full derivation of this result is given in Appendix B (Section B1) for any number of layers.

To model the shortwave radiation impacts of multiple layers, we then collapse the cloud layers into an equivalent single effective layer. To characterize this layer, we derive the effective asymmetry parameter of the overlapping system (Appendix B, Section B2). For *N* overlapping layers, this is calculated using the optical depth-weighted average value of the gamma function

$$\boldsymbol{\gamma_w} = \left(\prod_{\boldsymbol{i=1}}^{\boldsymbol{N}} \boldsymbol{\gamma_i}\right) \frac{\sum_{\boldsymbol{i=1}}^{\boldsymbol{N}} \boldsymbol{\tau_i}}{\sum_{\boldsymbol{i=1}}^{\boldsymbol{N}} \prod_{\boldsymbol{j\neq i}} \boldsymbol{\gamma_j}\, \boldsymbol{\tau_i}} \tag{6}$$

where τ_i and γ_i are the optical depth and gamma function ($1/(1-g_i)$) respectively for each individual layer. Using the effective gamma function, we can then derive R_c and R_c' as shown in Eq. (4) and (5) for the full stack of overlapping layers. Substituting (4), (5) and (6) back into Eq. (2), we obtain the radiative forcing components for *N* overlapping cloud layers as

$$\boldsymbol{RF_{SW,O}} = -\boldsymbol{S}\cdot\boldsymbol{t}\cdot(\mathbf{1}-\boldsymbol{\alpha})\frac{\boldsymbol{R_c}-\boldsymbol{\alpha R_c'}}{\mathbf{1}-\boldsymbol{\alpha R_c'}} \tag{7}$$

and then, this can be combined with the previously mentioned procedure for RF_{LW} (Fig. 2) applied to *N* overlapping cloud layers

$$\boldsymbol{RF_{LW,O}} = \boldsymbol{\varepsilon OLR_{clear}} - \left[\boldsymbol{OLR_{clear}}\prod_{\boldsymbol{i=1}}^{\boldsymbol{N}}(\mathbf{1}-\boldsymbol{\varepsilon_i}) + \sum_{\boldsymbol{i=1}}^{\boldsymbol{N}}\left[\prod_{\boldsymbol{j=i+1}}^{\boldsymbol{N}}(\mathbf{1}-\boldsymbol{\varepsilon_j})\right]\boldsymbol{\varepsilon_i}\boldsymbol{\sigma}^{*}\boldsymbol{T_i}^{\boldsymbol{k^*}}\right] \tag{8}$$

3.2 Input data for the radiative forcing model

3.2.1 CERM modeling tool

An hourly map of contrail optical depth, coverage and lifetime in 2015 is estimated using a global version of CERM (Caiazzo et al., 2017). CERM follows a bottom-up approach for simulating contrails by combining externally-provided meteorological and atmospheric data with flight track data.

With an hourly time-discretization, and a 0.25°×0.3125°×22 global grid, CERM estimates individual contrail properties (including optical depth and size) for all flights in a year using flight track and atmospheric composition data. CERM models contrails from formation to sublimation based on the physical evolution defined in Schumann (2012). Therefore, it is in theory capable of capturing linear contrails and contrail cirrus. Two contrails allocated in the same grid cell are assumed to be a single contrail while no interaction is assumed between contrails located at different vertical levels. Additionally, physical interactions between simulated contrails and natural clouds are not considered by CERM. This is in part because the contrails may form in the "non-cloudy" parts of grid cells, and in part because of uncertainty over contrail formation when flying through (for example) subvisible cirrus. We use meteorological reanalysis data from the GEOS forward processing (GEOS-FP) product, supplied by the NASA Global Modeling and Assimilation Office. Flight track and emissions data are calculated using the open-source Aviation Emissions Inventory Code (AEIC) (Simone et al., 2013).

The CERM version used to create the input data for this analysis incorporates new capabilities compared to previous versions (Caiazzo et al., 2017): a higher-resolution vertical grid (22 layers instead of 10 layers); a 4th order Runge-Kutta advection scheme; and an improved ice crystal coagulation model (Schumann, 2012).

3.2.2 Contrail-contrail and cloud-contrail overlap definition

CERM does not provide the position and orientation of contrails within each grid cell. As such, contrail overlap is computed by assuming the maximum possible overlap, which provides an upper-bound

estimate of total overlap. This approach assumes that the smallest contrail (by area) in each vertical column is fully overlapped with all other contrails in the column, repeating the process for all subsequent contrails in the column. If clouds are present in a vertical column, we assume that they are overlap with any contrails which are present, resulting in an upper bound estimate of overlap impacts.

A limitation of the CERM modeling approach is that contrails which form within the same hour, grid cell, and vertical layer (~350 m thick at cruise altitude) are aggregated into a single contrail layer. This means that overlap which would occur between contrails forming in close proximity is not included in our estimate of the effects of contrail-contrail overlap.

Typically in radiative forcing calculations in literature, clouds and contrails have been assumed to maximally overlap, either by reducing radiation reaching contrail layers or by modeling contrails as an increase in cloud fraction. This is consistent with the fact that cloud coverage is in general larger than contrail coverage. Contrail-contrail overlaps are assumed to occur randomly in most climate models where contrails are implemented, compared to true maximum overlap in this work and in CoCiP's RF calculations (Schumann et al., 2012). Ideally, additional information is provided regarding contrail orientation. In flight corridors where large numbers of aircraft pass within several hours of each other and with similar (or opposite) headings, overlapping, aligned contrails may be more common. However, this might not happen in denser flight areas like mainland US. Using information on flight paths to include contrail orientation in contrail modeling tools would be useful to more accurately model the impact of contrail-contrail overlaps on contrail-attributable radiative forcing. This and other avenues for improvement, such as through the use of higher vertical resolution, are discussed in Section 5.

3.2.3 Atmospheric radiation data

All atmospheric data required in the radiative forcing model are taken from observations by CERES instruments on three orbiting platforms (NASA Langley Research Center Atmospheric Science Data Center 2015). CERES data are provided on a 1°×1° resolution global grid at three-hour intervals. No interpolation is performed between estimates. This limitation is discussed further in Section 5.

The terrestrial, longwave radiation flux is simulated using the estimated "clear-sky" outgoing longwave flux provided by CERES. The "clear sky" flux is the estimated flux in the absence of clouds. This removes the need to estimate outgoing fluxes based on indirectly-observed surface temperatures. Longwave emission from cloud layers is calculated as described in Corti and Peter (2009). The total incident shortwave radiation S is computed using the solar zenith angle calculated based on time and geographic location (Kalogirou, 2014) as

$$S = S_0 \left(1 + 0.033 \cos\left(2\pi \cdot \frac{J}{365}\right)\right) \mu, \quad (9)$$

where S_0 is the solar constant (1366.1 W/m^2), μ is the cosine of the solar zenith angle θ, and J is the Julian Day.

3.2.4 Natural cloud data

CERES instruments also provide data on natural cloud coverage, with clouds detection based on Minnis et al. (2008) algorithms. These are divided into four vertical levels defined by pressure, and include cloud properties such as optical depth and temperature. We use this data to estimate natural cloud cover when calculating the impacts of contrails in 2015. The detection limit of the CERES instruments has been estimated in the past as approximately $\tau = 0.02$ (Dessler and Yang, 2003), while later studies comment on thresholds closer to $\tau = 0.05$ (Kärcher, 2009).

Since CERES instruments provide data on only the sum of detected clouds (including visible contrails), we may be double counting the influence of contrails. Four levels of clouds are given in CERES data, defined by their pressure level and corresponding to the following altitudes: from 0 to 10,000 ft, from 10,000 ft to 16,500 ft, from 16,500 ft to 30,000 ft, and above 30,000 ft. Accordingly, most contrails would appear in the 4th level detection.

There is a high-level cloud in the same location as a CERES detectable contrail (optical depth higher than 0.02) in 58% of contrail cases, whereas only 6% of contrails occupy the same level as mid-level clouds (3rd CERES vertical level). There is in theory the possibility that ~60% of all contrails are already accounted for in the CERES data. However, the detection limit of the CERES instruments is approximately $\tau = 0.02$ (or up to 0.05 from later studies). Considering that the average optical depth from CERM for 2015 global contrails is 0.065, a significant fraction of CERM contrails are not detectable by CERES instruments. Additionally, satellite detection limits do not affect our contrail coverage data meaning that this study includes subvisible contrails in impact and RF calculations.

Contrail cirrus has the potential of modifying the properties of natural cloud coverage by changing the availability of atmospheric water. We assume that this effect is already captured by the natural cloud data retrieved by CERES for year 2015. This impact has been estimated in the past to reduce global contrail radiative forcing by approximately a fifth (Burkhardt and Kärcher 2011) and by 15% (Schumann et al., 2015).

3.3 Experimental design

We analyze the radiative forcing impacts of cloud-contrail and contrail-contrail overlaps using a three-step approach.

In the first step, through a parameterized analysis, we quantify the effect of a two-layer overlap on total radiative forcing when compared to a case where the layers are assumed to be independent, calculating how the effect of overlap varies as a function of the layer properties and the local conditions. This analysis shows the conditions under which the RF of two overlapping contrails is significantly different to the total RF of two independent contrails. This nonlinearity is representative of the existing bias in estimated contrail RF values found in the literature.

In the second step, we evaluate the global sensitivity of contrail RF to cloud-contrail and contrail-contrail overlaps using 2015 atmospheric data (meteorology and natural clouds). We calculate the RF associated with one or two contrail layers at each global location for one day from each month of the year in order to capture seasonal variation. To demonstrate this, we simulate a case used previously in estimates of contrail-attributable radiative forcing (Myhre et al., 2009; Schumann et al., 2012). The RF attributable to a hypothetical contrail is calculated for each location globally assuming typical optical properties (g = 0.77), optical depth (0.3), and altitude (around 10.5 km). In order to quantify the effect of cloud overlap we evaluate radiative forcing with and without natural cloud cover ("all sky" vs. "clear sky"). By subtracting the RF obtained in the "clear sky" scenario from the RF obtained in the "all sky" scenario, we obtain the difference in contrail RF attributable to the presence of clouds. The results can then be linked to different cloudiness conditions to systematically analyze the impact of cloudiness on contrail RF. In order to quantify the global sensitivity to contrail-contrail overlaps we simulate a superposition of two contrail layers at each location, separated by a vertical distance of approximately 0.5 km.

Finally, we quantify the effect of cloud-contrail and contrail-contrail overlap on the global contrail-attributable RF in 2015. We use year-2015 contrail coverage data obtained from CERM (Caiazzo et al., 2017) and analyze the associated radiative forcing impacts for the four scenarios shown in Table 4.

Table 4. Scenarios analyzed for 2015 global contrails.

	Cloudiness Assumption	
Contrail overlap assumption	**Clear sky (no clouds) (C)**	**All sky (clouds) (A)**
Independent (I)	IC	IA
Overlapping (O)	OC	OA

Global evaluations are performed using detailed contrail coverage estimates and meteorological data described in Section 3.2.

4 Results

4.1 The effect of overlap on contrail-attributable radiative forcing in a single column

In this section we evaluate the general effect of overlap on contrail RF through a parameterized analysis. We simulate two overlapping layers with different optical depths (τ) and temperatures (T) (either natural cloud or contrail). By varying the layer properties, we are able to simulate both cloud-contrail and contrail-contrail overlaps. We also evaluate the effect of solar zenith angle (θ), estimated outgoing longwave radiation without clouds (OLR_{clear}), and Earth surface albedo (α).

The contrail modeling and observation literature suggests that contrails are usually optically thin, with typical optical depths in the range 0 to 0.35 (see Table 1). They also form almost exclusively at cruise altitude. Natural clouds are located within a greater range of altitudes and can achieve greater optical depths. We simulate contrail layers over a range of depths ($0 < \tau < 0.5$), based on typical values, at low temperatures/high altitudes (210 – 230 K), and with an asymmetry parameter of 0.77, representative of mature contrails (Heymsfield et al. 1998; Febvre et al., 2009; Markowicz et al., 2011a; Gayet et al., 2012; Schumann et al., 2017; Febvre et al., 2009; Gayet et al., 2012; Sanz-Morère et al, 2020). Cloud layers are simulated as being thicker ($0 < \tau < 4$), at higher temperatures/lower altitudes (215 – 280 K), and with an asymmetry parameter of 0.85, corresponding to low level clouds. When not otherwise specified, we assume each contrail layer to have an optical depth τ of 0.3 and temperatures of 215 K (upper) and 220 K (lower). This optical depth is at the upper bound of literature estimates of typical values for contrails (Voigt et al., 2011). For this analysis natural cloud layers are assumed to have an optical depth τ of 3 and a temperature of 260 K. The prescribed outgoing longwave radiation in this single-column analysis is 265 W/m^2 (consistent with a ~288 K surface temperature), with an albedo $\alpha = 0.3$ and solar zenith angle $\theta = 45^o$.

The total forcing for the combined, overlapping layers is calculated as shown in Section 3.1. We calculate the "independent" forcing as the RF that would have been calculated by adding together the RF from each layer independently, without accounting for any overlap. We evaluate the effect that overlap has on the

contrail-attributable net radiative forcing in both systems (cloud-contrail and contrail-contrail) as a function of each parameter. We then estimate the bias in estimated RF that results if overlap is ignored, as is typically the case in existing contrail modeling. We also evaluate contrail RF when surrounded by cirrus clouds and finally, we validate our overlap model comparing it with the FL96 model previously described (Liou, 1986; Fu and Liou, 1993; Fu, 1996).

4.1.1 Parametric analysis of cloud-contrail and contrail-contrail overlap effects on contrail-attributable net RF

The effect of overlap on contrail-attributable RF depends both on cloud layers' properties and on local conditions. We first evaluate how the effect of overlap varies with cloud layer properties, including thickness of the two layers. We then quantify the effect of local conditions: solar zenith angle (θ), estimated outgoing longwave radiation in clear sky conditions (OLR_{clear}), and Earth surface albedo (α).

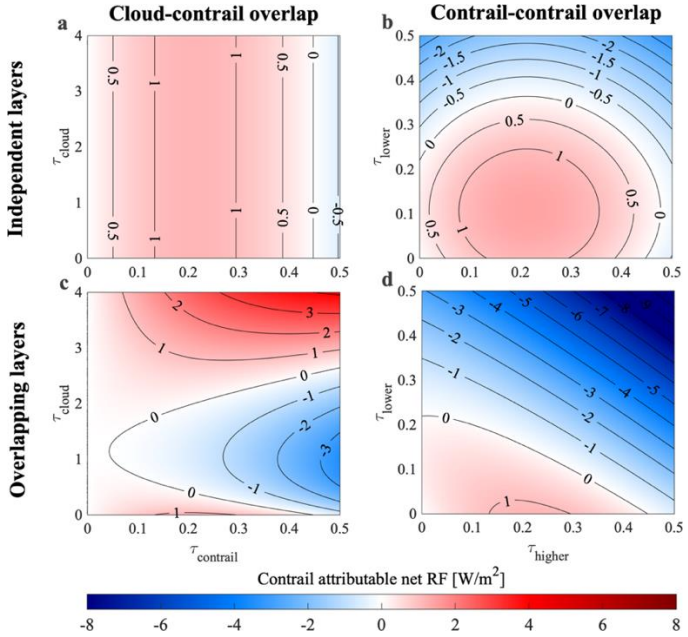

Figure 2. Effect of overlap between two layers on the contrail-attributable net RF as a function of optical depth τ. Left: RF attributable to a single contrail when overlapping with a natural cloud layer. Right: total RF in a system of two overlapping contrails. Top: contrail RF estimated when treating the layers as independent and summing individual contributions. Bottom: contrail RF estimated in a single calculation which accounts for overlap. Negative RF is shown in blue and positive RF is shown in red. Contrail properties are: asymmetry parameter of 0.77, temperature of 220 K and 215 K respectively. Cloud properties are: asymmetry parameter of 0.85, temperature of 260 K. The solar zenith angle θ = 45° for all calculations. An additional version of this figure, calculated using a solar zenith angle θ = 30° and covering a greater range of optical depths, is provided as Figure S3 for comparison to other literature.

We evaluate the effect of overlap on contrail-attributable net RF for both cloud-contrail (with the contrail at 215 K) and contrail-contrail (at 215 K and 220 K) systems. The variation in contrail-attributable net RF with optical depth of either layer is shown in Figure 2. A decomposition of the results in terms of longwave and shortwave components can be found in the SI (figures S1 and S2). The panels on the left show the effects of cloud-contrail overlap, while those on the right show the effects of contrail-contrail overlap. The upper row shows the net RF when the layers are considered to be independent, while the bottom row shows the RF when accounting for interactions between the two (i.e. overlap). Each panel shows the net, contrail-attributable RF of the system (i.e. subtracting only any RF which is calculated when no contrails are simulated).

The RF attributable to a single contrail (no overlap) as a function of its optical depth is shown in the upper left panel (Fig. 2a). This is because, when overlap is ignored, the contrail-attributable RF of a cloud-contrail system is equal to the RF of the contrail alone. The RF increases from zero to a maximum of ~1.2 W/m^2 as the optical depth increases to ~0.2, after which increasing depth instead results in reduced RF. This is due to the compensation of the increase in absorption by the increase in reflectance with increasing optical depth. The lower left panel (Fig. 2c) then shows how the presence of a cloud layer affects contrail-attributable RF as a function of the optical depth of each layer. The presence of a (lower) natural cloud layer can either increase or decrease the contrail-attributable RF depending on the optical depth of the cloud layer. Thin clouds can transform a warming contrail into a cooling one by absorbing part of the longwave radiation that previously reached the contrail. Thick clouds can transform a cooling contrail into a warming one (from a net RF of -0.54 W/m^2 to +4.1 W/m^2 at a contrail optical depth of 0.5) by mitigating the shortwave cooling of the contrail. These results explain the existing uncertainty related to the effect of natural clouds on contrails' radiative impact. If overlap between the layers is ignored (Fig. 2a), these features are not captured.

Figure 3d shows the effect of contrail-contrail overlaps on contrail-attributable RF. The effect of each contrail individually can be seen based on the values along the left and lower edges. The lower contrail, due to its higher temperature (less LW absorption), becomes cooling at a lower optical depth of ~0.22

(compared to ~0.45 for the upper contrail). The effects of overlap are similar to the effects obtained when a thin cloud ($\tau \sim 0.1$) is overlapping with a contrail: the net effect of increasing the optical depth of the contrail is to make the system more cooling (Fig. 2d). However, since both layers are artificial (contrails), increasing the optical depth of either layer yields a more negative RF, unlike the case of a thick natural cloud with a thin contrail. This is because the shortwave cooling attributable to contrails increases regardless of which layer is providing the shortwave cooling. This results in a monotonic decrease in warming (increase in cooling) attributable to the net contrail-attributable RF, from +1.2 W/m^2 for a single contrail of optical depth 0.25, to -10 W/m^2 for two contrails both of optical depth 0.5. For comparison, Figure 2b (upper right panel) shows the result when RF is calculated based on the independent combination of each contrail's RF. Independent calculation gives the wrong response by neglecting the screening effect on longwave radiation by the lower contrail. This error is small for low contrail thicknesses, with a maximum difference of -1.0 W/m^2 for a total contrail-contrail system thickness below approximately 0.15. However, for thicker contrail layers, both the sign and magnitude of the net effect can be incorrectly predicted when overlap is neglected. This analysis also confirms the findings of Kärcher and Burkhardt (2013) with regards to the overestimation of contrail RF by prescribing a mean optical depth. As an example, two simulated overlapping contrails of optical depths 0.1 and 0.2 result in ~0.8 W/m^2 of radiative forcing, but two overlapping contrails of optical depth 0.15 result in a forcing of 1.1 W/m^2).

The altitude (temperature) of each layer also affects the effect that overlap has on the net contrail-attributable RF. Net attributable RF of a contrail-contrail system decreases as contrail altitude decreases (increasing temperature), due to the increase in the temperature of re-emission. For a cloud-contrail system, the contrail-attributable RF is most sensitive to the altitude (temperature) of the natural cloud. The absolute difference varies from +6.1 W/m^2, for warmer (lower-altitude) clouds, to -12 W/m^2, for cooler (higher) clouds, assuming an optical depth of 3 for the natural cloud layer (see Fig. S4 in the SI).

The radiative forcing attributable to contrails (as well as the effect of overlap) also varies as a function of local conditions, such as the outgoing longwave radiation (related to surface temperature), surface albedo, and solar zenith angle. The greatest contrail-attributable warming occurs for high values of outgoing (terrestrial) longwave radiation, and high surface albedos. This is due to the combination of increased longwave radiative forcing and the reduced shortwave cooling from the contrail. We also find that the net RF of the contrail-contrail system is reduced as the solar zenith angle increases. As θ increases from 0º to 75º, the maximum net RF (at maximum OLR_{clear} and α) decreases from 27 W/m^2 to 8.0 W/m^2. This effect, driven by changes in the shortwave cooling, is explored in more detail in Appendix B (Section 3). The relative effect of overlap on both the warming and cooling components of contrail-attributable RF is, in relative terms, insensitive to outgoing longwave radiation and albedo. Due to the low absolute values of $|RF_{SW}|$ at maximum α and high values of $|RF_{LW}|$ at maximum OLR_{clear}, maximum absolute net RF decrease happens in those areas. For a deeper analysis, figure S5 in the SI shows the variation of net RF in a contrail-contrail overlap event, with OLR_{clear} and α.

4.1.2 Parametric analysis of contrail-contrail overlap specific impact on RF_{SW} and RF_{LW}

We now evaluate the error in both RF_{SW} and RF_{LW} which results from ignoring the effect of contrail-contrail overlap. We use RF_O to denote the RF when overlap is treated explicitly and RF_I to denote when overlap is ignored ("independent"), in which case the total RF is the sum of the RF from each cloud layer. The relative change in the estimated RF impact of the system is then

$$D = \Delta RF = \frac{(RF_I - RF_O)}{|RF_O|} \quad (8)$$

where a positive value of D indicates that the assumption of independence results in an overestimate of warming effects (LW) or an underestimate of cooling effects (SW). Equivalently, a positive value means that accounting for overlap results in a decrease in the RF of the system relative to the independent calculation.

Figure 3 shows the percentage bias resulting from ignoring overlap when quantifying the RF of a contrail-contrail system. This is quantified as a function of each contrail's optical depth and of the local solar zenith angle (θ). In each case, the upper and lower contrail have identical physical properties, as described in Section 4.1.1. We find that accounting for overlap consistently results in a reduced longwave RF for two overlapping contrail layers. This means that, if overlapping contrails are considered as independent, their longwave RF is overestimated by up to 16% (for contrails with optical depth of 0.5). This effect is independent of the solar zenith angle.

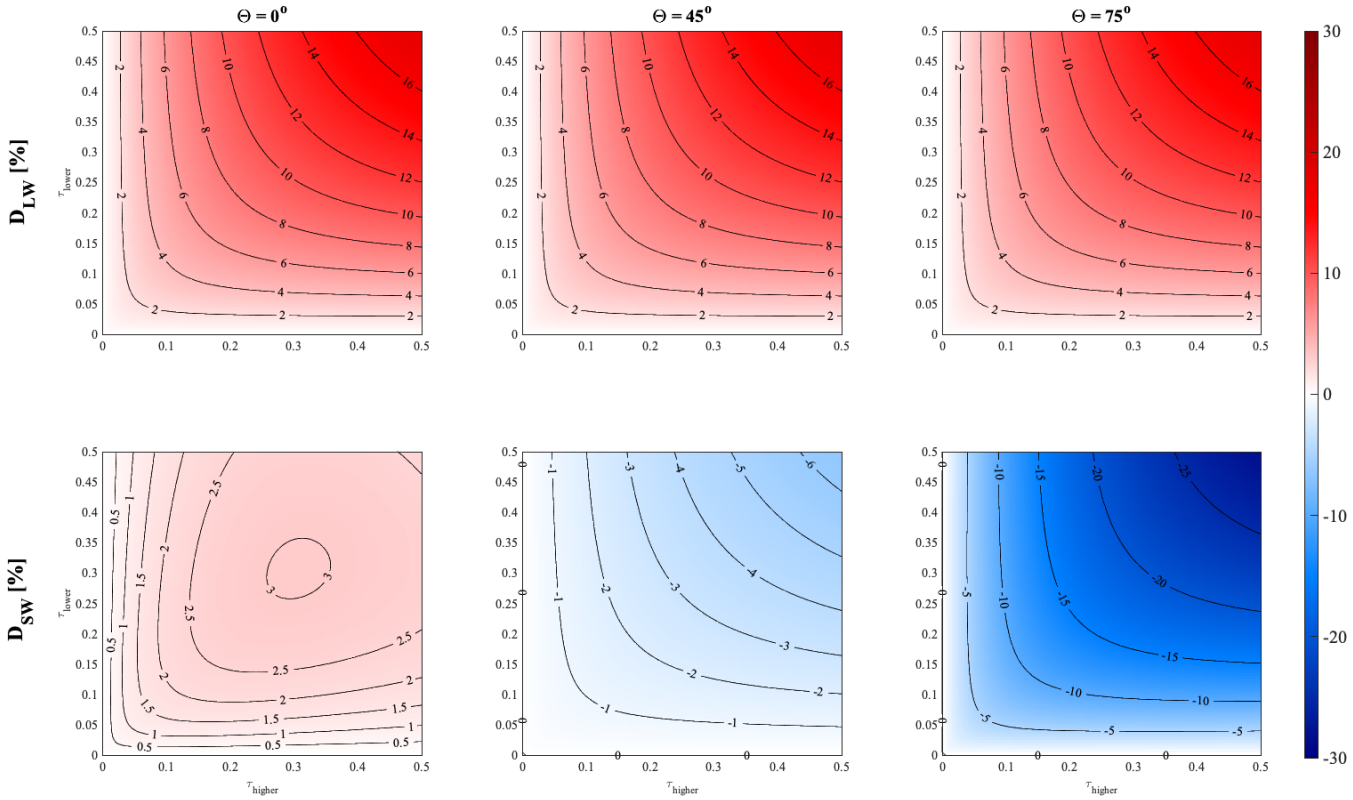

Figure 3. Error in estimated RF for two overlapping contrails when ignoring interaction, as a function of τ and θ. The solar zenith angle increases from the left-most to right-most panels. The upper panels show longwave RF error, while the lower panels show shortwave RF error. Positive (red) values indicate that the independent assumption results in an overestimate of warming effects (or underestimate of cooling effects). Negative (blue) values indicate that the independent assumption results in an overestimate of cooling effects (or underestimate of warming effects). An additional version of this figure, including calculations using a solar zenith angle θ = 30° and covering a larger range of contrail optical depths, is provided as Figure S6 for comparison to other literature.

For shortwave RF, the error resulting from independent calculation is sensitive to the solar zenith angle. In most cases, the total shortwave ("cooling") RF is smaller in magnitude when correctly accounting for overlap, relative to the independent calculation. This corresponds to an overestimate of the total reflectance if contrails are treated as independent. The magnitude of this error generally increases with contrail optical depth. Near sunrise or sunset ($\theta \approx 75°$), accounting for overlap reduces the calculated cooling effect by 25% for $\tau = 0.5$. However, we observe a change in the sign of the error at zenith angles below ~25°. At noon ($\theta = 0°$), assuming independent effects results in a slight underestimate of the cooling effect for any optical depth between 0 and 0.5, up to a value of 3.2%. The cause for the change in sign at very low solar zenith angles is investigated in detail in Appendix C.

The effect on total net RF depends on the tradeoff between the effects on both RF_{LW} and RF_{SW}. At low solar zenith angles, neglecting contrail-contrail overlaps results in an overestimation of net RF. Due to the changes in sign of the error for shortwave RF, and the fact that the magnitude of each of the two components varies based on different factors, the effect on net RF at high solar zenith angles will depend on factors such as the location, time, and properties of each contrail.

In summary, we find that the net radiative forcing due to contrails may include a significant non-linear term due to overlap which is not captured in existing models. For contrails with optical depths of up to 0.5, we find that failing to account for this non-linearity could result in an overestimate of both the longwave warming (up to 16%) and the shortwave cooling (up to 25%). The sign and magnitude of the effect on the system net RF is highly dependent on layers' properties, local conditions, and the solar zenith angle. The total effect of overlapping on a single contrail is therefore dependent on the solar zenith angle (time), temperature (altitude), and geographic location in which the contrail is formed.

4.1.3 Parametric analysis of radiative impact from a contrail located in-between cirrus clouds

We also model the case of a single contrail located between two natural cirrus cloud layers. We simulate a single contrail with the same properties as were used in the previous section (temperature of 215 K, optical depth of 0.3, and asymmetry parameter of 0.77). This is bracketed by two cirrus clouds, 500 m

above and below the contrail, with optical depths of up to 1.5 and an asymmetry parameter of 0.75 (Kokhanovsky, 2004).

Figure 4 shows how the single contrail RF varies as a function of the optical depth of both natural cirrus clouds and as a function of solar zenith angle. For reference, the estimated RF for the contrail at a solar zenith angle of 45° in the absence of clouds is +27.9 W/m^2 (longwave) and -26.9 W/m^2 (shortwave), resulting in a net forcing of 1.0 W/m^2.

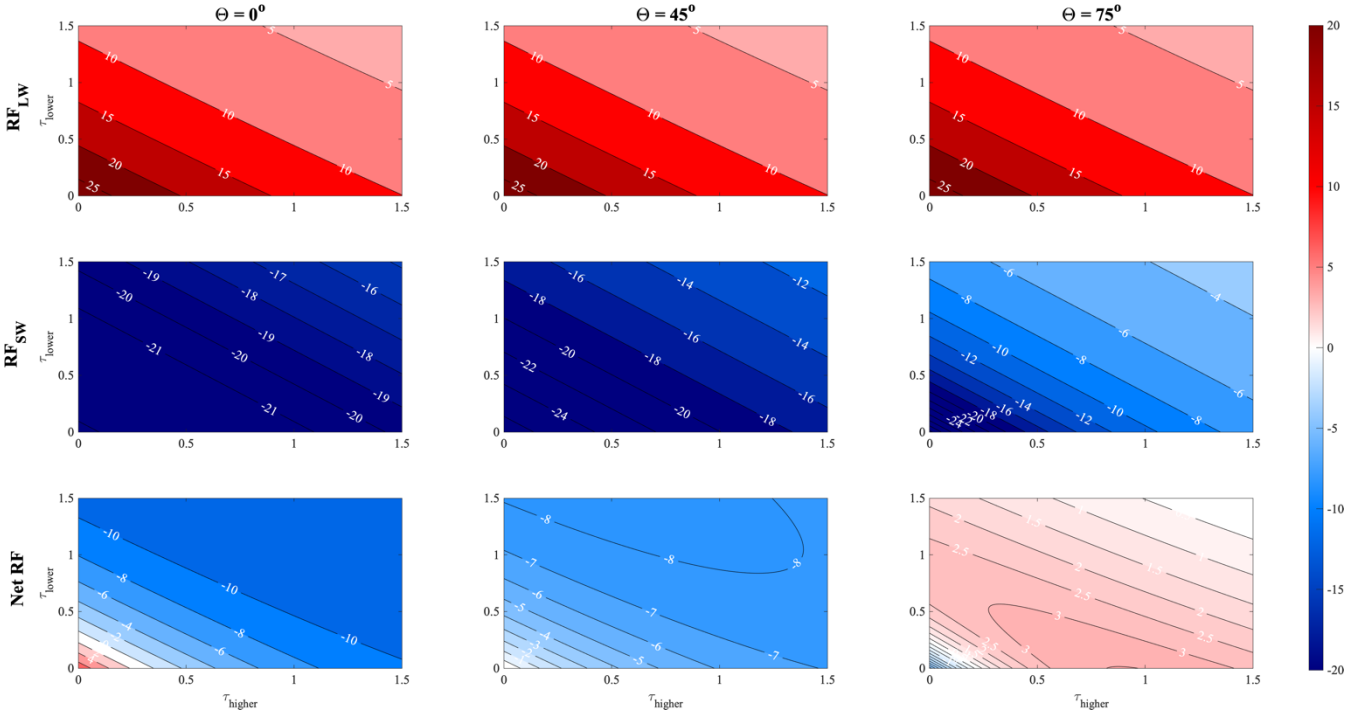

Figure 4. Radiative forcing [W/m^2] due to a single contrail between two cirrus cloud layers. Radiative forcing is shown as a function of the solar zenith angle (increasing from left to right) and the optical depth of the lower (Y-axis) and upper (X-axis) natural cloud optical depths. From top to bottom: longwave; shortwave; and net radiative forcing. Contrail optical depth τ = 0.3. An additional version of this figure, including calculations using a solar zenith angle θ = 30° and using a smaller contrail optical depth, is provided as Figure S7 for comparison to other literature.

The presence of either cloud layer alone decreases both the longwave and shortwave RF attributable to the contrail, as previously discussed. Except at high solar zenith angles, increasing the optical depth of either cloud layer reduces the net RF of the contrail layer. This is because the contrail's longwave RF falls rapidly, while the shortwave RF is less affected. The contrail's longwave radiative forcing decreases

by up to a factor of seven when the surrounding clouds are sufficiently thick ($\tau = 1.5$), while the shortwave radiative forcing is only reduced by a factor of three. However, at high solar zenith angles, this situation is reversed (see Figure B2 in Annex B). This means that the contrail RF instead initially increases with increasing cloud thickness.

4.1.4 Validation of the overlap model

In addition to validating the model for the purposes of simulating a single contrail (Section 3.1.2), we also compare the model's estimates of the effect of two-layer overlap to estimates from an existing radiative transfer model - the previously-described Fu-Liou radiative transfer model (FL96). FL96 uses solid hexagonal columns to represent ice clouds, which have previously been found to be best represented in the Corti and Peter model by assuming an asymmetry parameter $g = 0.87$ (Corti and Peter, 2009). Figure 5 shows the error resulting from considering overlapping contrails as if they were independent, for both longwave and shortwave components, in both models. All simulations are performed using identical radiation data (outgoing longwave radiation and land albedo) and contrail properties. More information is provided in Appendix A.

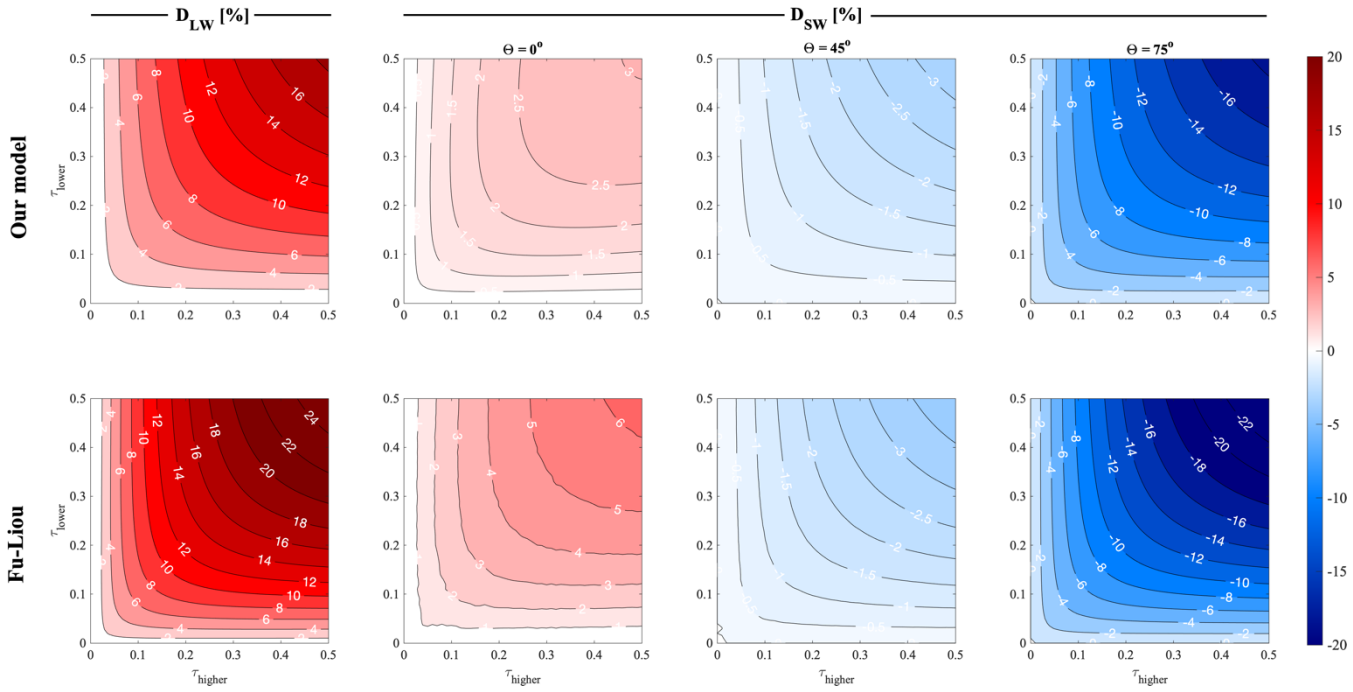

Figure 5. Error in estimated RF for two overlapping contrails when ignoring interaction, as a function of τ and θ, for both our model (upper row of panels) and FL96 (lower row of panels). The first column shows error in longwave RF, while the remaining columns show error in shortwave RF at different solar zenith angles. Positive (red) values indicate that the independent assumption results in an overestimate of warming effects (or underestimate of cooling effects). Negative (blue) values indicate that the independent assumption results in an overestimate of cooling effects (or underestimate of warming effects). An additional version of this figure, including calculations using solar zenith angles θ = 15°, 30° and 60° is provided as Figure S8 for comparison to other literature.

Qualitatively, the behavior is consistent between the two models. Both models estimate that the discrepancy in simulated longwave and shortwave RF (comparing the "overlap" to "independent" cases) increases with the increasing optical depth of each cloud layer. We also observe the same reversal of sign in the shortwave error at very low solar zenith angles. FL96 finds that both errors increase more quickly with optical depth than is estimated by our model, finding a maximum error in longwave RF of 25% (17% in our model) and in shortwave RF of 24% (18% in our model). This indicates that our model correctly represents overlapping behavior but might underestimate the effect on both terms. The net RF difference is always lower than 30% and varies with solar zenith angle. At low solar zenith angles we underestimate net RF (both for two independent and overlapping contrails). At θ = 45° we obtain the best agreement, with differences lower than 10% and at θ = 75° we overestimate net RF by up to 30% at an optical depth,

for both contrails, of 0.5 (at the upper end of current contrail optical depth estimates). These differences must be considered in the context of the global net RF results presented in Section 4.3.

4.2 Global sensitivity of cloud-contrail and contrail-contrail overlap to location and season

We next quantify the variation of contrail radiative forcing as a function of geographic location and time of year. This captures the primary drivers in variations regarding the effects of overlap, as identified previously.

To obtain these sensitivities, we run a global simulation using 2015 atmospheric data (including radiation and natural cloudiness data as described in Section 3.2) in which we simulate the presence of a contrail layer in each location across the globe. We here assume that, in each grid cell, 1% of the total area is covered by contrail, reproducing an analysis performed by Schumann et al. (2012). We evaluate the effect of both cloud-contrail and contrail-contrail overlaps on contrail-attributable RF. We also calculate the error which would be incurred by treating two overlapping contrails as independent.

Figure 6 shows the radiative forcing per unit of additional contrail optical depth at each location, under both “clear sky” and “all sky” conditions (without and with natural clouds respectively, for year-2015 natural cloud cover). The RF varies as a function of latitude, consistent with prior studies (Schumann, 2012). The longwave warming (RF_{LW}) is maximized in regions with higher surface temperatures such as the equator. Cooling (negative RF_{SW}) is instead sensitive to surface albedo, being maximized over oceans and minimized over snow-covered or desert regions.

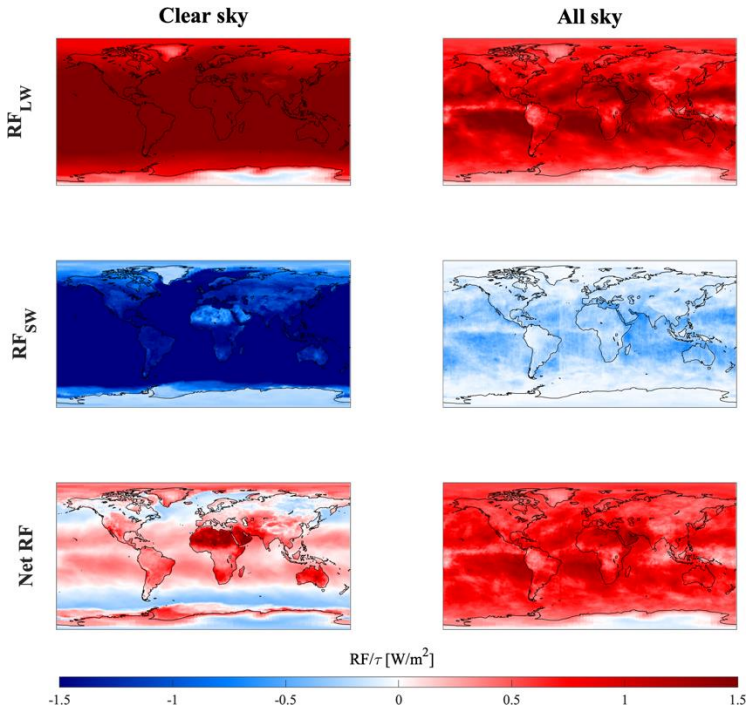

Figure 6. Hourly average radiative forcing per unit optical depth [W/m^2] for a 1% contrail covering per 0.25°× 0.3125° cell and g=0.77 (2015 atmospheric data) From top to bottom: Longwave, shortwave, and net RF. Clear sky sensitivities are shown on the left, and all sky calculations on the right. Small discontinuities in shortwave cooling for all-sky conditions (e.g. over the North Atlantic Ocean) are the result of data artifacts in the CERES satellite data, which is a composite of observations from multiple observation platforms.

By comparing the "all-sky" and "clear-sky" simulation results, we find that the absolute value of both components of radiative forcing is reduced by the presence of clouds. The global mean reduction in shortwave forcing (~83%) exceeds the reduction in longwave forcing (~42%), meaning that cloud overlap causes a more than three times increase in the global, area-weighted average, contrail-attributable net RF, from +27.8 mW/m^2 to +107.1 mW/m^2 per unit of contrail optical depth. These values are consistent with prior studies (e.g. Schumann et al. 2012).

Our assumed asymmetry parameter for each contrail layer (g = 0.77) corresponds to a greater backscatter than is the case in previous studies (Fu and Liou, 1996; Myrhe et al., 2001; Schumann et al., 2012). This explains the low global sensitivity obtained in clear-sky conditions. For comparison, using an asymmetry parameter of g = 0.9 (typical of regular, spherical particles) results in a global mean, clear-sky sensitivity of +144.3 mW/m^2, reducing cloud-contrail global impact. A deeper analysis of uncertainty related to

microphysics and resulting global sensitivity to contrail is the subject of a complementary work (Sanz-Morère et al., 2020).

At night this effect reverses, as the reduction in reflected shortwave radiation is lost while the reduction in absorbed longwave radiation remains. The global, area-weighted average nighttime contrail-attributable RF is therefore reduced by 42% when accounting for the presence of clouds. However, these effects vary significantly with geographic location.

The depth, frequency, and altitude of natural cloud cover all vary as a function of location, resulting in a geographical dependence of the sensitivity of contrail RF with respect to clouds. Thick, low altitude clouds are more common at midlatitudes, while higher, thinner cirrus clouds are more common in the tropics (Warren et al., 1988; Sassen et al., 2008; Marchand et al., 2010). The effect of these clouds on contrail RF is shown in Figure 7. In the tropics (TROP, 30°S - 30°N), contrail RF is 1.5 times higher in the presence of clouds. However, in the midlatitudes (MLAT, 30°N - 60°N), the thicker, warmer clouds have a greater effect. Overlap with midlatitude clouds increases the net RF attributable to a contrail by more than a factor of six, from 8.7 mW/m^2 to 66 mW/m^2. This result is consistent with the analysis given in Section 4.1.1, and is due to the high reflectivity of the thick, low-altitude clouds.

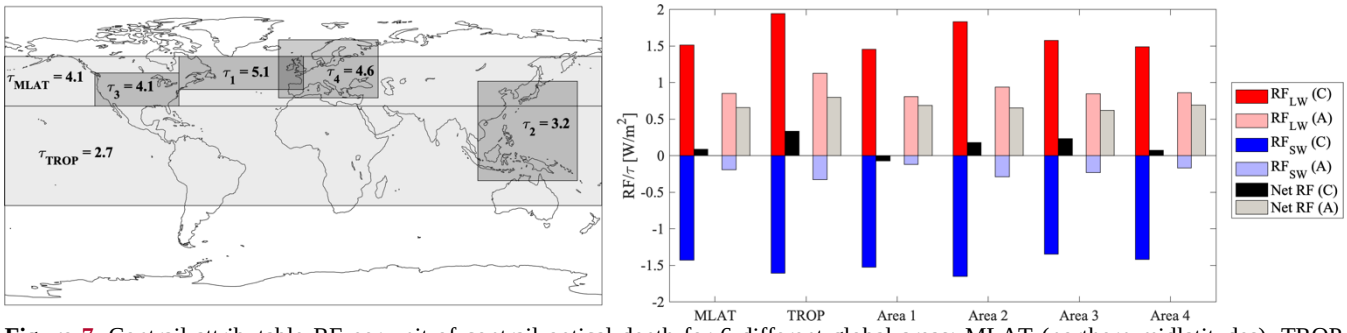

Figure 7. Contrail-attributable RF per unit of contrail optical depth for 6 different global areas: MLAT (northern midlatitudes), TROP (tropics), and subregions 1-4. Left panel: latitudinal and longitudinal limits and average natural cloud optical depth of each area. Right panel: average RF per unit of optical depth per area (A: all sky, C: clear sky)

We also quantify the sensitivity of contrail RF to overlap in four different geographical subregions: area 1, representing the North Atlantic corridor; area 2, which includes parts of Asia; area 3, approximately representing the continental United States; and area 4, approximately representing Europe (see Figure 7).

These areas include ~53% of all passenger traffic in 2017 (Boeing, 2018) and differences in sensitivity for each region provide insights into the effects of future growth.

In all four regions, clouds have a greater relative and absolute effect on shortwave RF than on longwave RF (Figure 7). In area 3, clouds reduce the longwave RF per unit contrail optical depth by 46%, while reducing the shortwave RF by 83%. This results in 2.3 times increase in the net RF relative to the clear-sky case. By contrast, in the North Atlantic corridor (area 1), clouds reduce the longwave RF by 44%, but the shortwave RF is reduced by 99%. This changes a cooling effect of 70 mW/m^2 into a warming of 690 mW/m^2. The effects of cloud overlap in areas 2 and 4 lie in between these two extremes.

These variations are driven by differences in natural cloud coverage (primarily due to latitude) and surface albedo (e.g. land vs. sea). In the case of area 1, contrails are mostly forming over water, which has a very low albedo. As a result, there is a larger shortwave cooling, and therefore a greater increase in the net RF when this cooling is mitigated by overlap with clouds. By contrast, over area 3 there is a greater land fraction and the clouds are thinner, resulting in a smaller overlap effect. These results suggest that avoiding overlap of contrails with clouds will yield the greatest RF reduction on midlatitude, oceanic routes, whereas the advantages of doing so over land and/or at lower latitudes will be smaller.

Contrail RF, and its sensitivity to clouds, also varies by season. Under all-sky conditions, in the Northern Hemisphere, the net contrail sensitivity is globally 15% lower in local winter than in local summer. This is because the reduction in longwave RF due to cooler surface temperatures exceeds the reduction in shortwave RF from shorter days (less insolation). However, this varies significantly by latitude because of the effect of changes in day length.

Climate change is likely to affect these results due to its effects on global cloud cover (Norris et al., 2016). Current satellite data show that cloud top heights are gradually increasing, which will likely decrease contrail net RF due to the resulting decrease in cloud top temperature. It is also anticipated that the tropics

will expand (Kim et al., 2017). This will mean that more contrails are overlapping with high-altitude clouds, resulting in a reduced sensitivity to cloud overlap as discussed earlier.

We also evaluate how the effect of contrail-contrail overlap on contrail-attributable RF varies by location. This is quantified by simulating two contrail layers at each location, first treating them as independent and then calculating the total RF when accounting for overlap. The layers are simulated as being separated by 500 m. We find that correctly accounting for overlap results in a decrease in both the cooling and warming effects, relative to the "independent" calculation. The percentage decrease in each component is approximately uniform across all locations (consistent with Section 4.1.1). Since the components are of opposite sign, this results in a non-uniform effect on total net RF. Contrail overlap has the greatest effect on the net RF when contrails are located in hot, equatorial areas (increased longwave RF) with high albedo (reduced negative shortwave RF), as is the case in low-latitude desert areas such as the Sahara. This results in a maximum contrail attributable net RF reduction by contrail-contrail overlapping in the tropics (TROP), where we find a reduction from an average sensitivity of 1.6 W/m^2 (per unit of optical depth) for two "independent layers" to an average sensitivity of 0.6 W/m^2 for two "overlapping layers". Global sensitivity maps to contrail-contrail overlap are shown in Figure S9 of the SI.

4.3 Effect of cloud-contrail and contrail-contrail overlaps on net 2015 global radiative forcing attributable to contrails

Finally, we quantify the net effect of cloud-contrail and contrail-contrail overlap for existing aircraft traffic patterns. We use year-2015 contrail coverage data as estimated using CERM (see Section 3.2.1). The RF impacts of contrails are presented in Table 5, under all-sky and clear-sky conditions, and with and without explicit treatment of contrail-contrail overlap.

4.3.1 Cloud-contrail overlaps

For 2015, we find that approximately 75% (by area) of contrails overlap with mid-level clouds. We compare results calculated under all-sky and clear-sky conditions (scenarios OA and OC) to quantify the effect of cloud-contrail overlap on contrail-attributable RF.

Figure 8 shows the effect of cloud-contrail interactions on the shortwave and longwave radiative forcing due to contrails. We find a 66% decrease in net global cooling attributable to contrails as a result of cloud cover, accompanied by a 37% decrease in warming. Accounting for cloud interactions therefore results in more than ten times greater net contrail-attributable warming. As a consequence, the annual average, global net RF changes from +0.7 mW/m^2 under clear sky conditions to +9.7 mW/m^2 when including clouds ("all-sky"). Overlap with clouds is found to reduce the global longwave RF of contrails by 37%, and the shortwave RF by 66%. At night, contrails over natural clouds have a lower net RF due to the lack of any shortwave effect. As a result, the presence of natural clouds during nighttime reduces the net RF of contrails by 37% as the only effect that clouds can have at this time is to mitigate the contrail-attributable longwave RF.

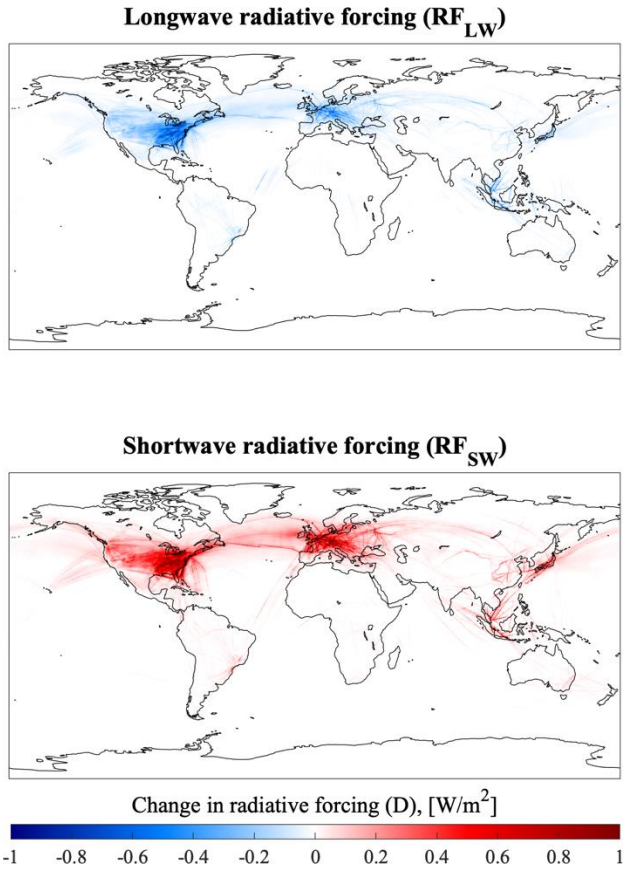

Figure 8. Change in annual-average RF [W/m^2] due to the presence of clouds from global flights in 2015. Upper panel: Longwave RF (blue corresponds to negative, meaning that clouds reduce the warming effect of contrails). Lower panel: Shortwave RF (red corresponds to positive, meaning that clouds reduce cooling effect of contrails).

4.3.2 Contrail-contrail overlaps

An analysis of year-2015 global contrail coverage simulated at a resolution of 0.25°×0.3125° using the CERM modeling tool (Caiazzo et al., 2017) provides an estimate of overlap frequency. Assuming maximum overlap by area (i.e. all contrails in a given column overlap to the greatest possible extent, see Section 3.2.2), up to 15% of all contrail area includes overlap with other contrails (Fig. 9, lower plot). More details on this assumption and the CERM modeling tool are given in Section 3.2. The majority of this overlap occurs for contrails which are no longer line-shaped, and which may appear to be natural cirrus when viewed from the ground. If we exclude contrails which are more than an hour old or which are "subvisible" for human eye, having an optical depth below 0.03 (Kärcher, 2002; Kärcher, 2018), this fraction falls to 2.2%.

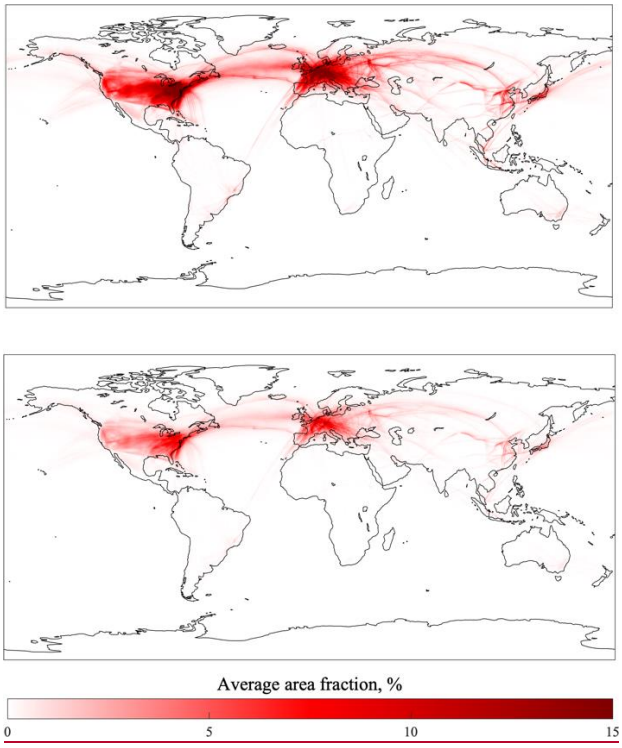

Figure 9. Estimated annual mean global contrail coverage for 2015. Upper panel: yearly average contrail coverage (in %), assuming no contrail-contrail overlap. Lower panel: yearly average coverage (in %), assuming "maximum overlap" such that all contrails in a single column are centered in each 0.25°×0.3125° grid cell (in %). Contrail data were generated using the CERM global contrail modeling tool (Caiazzo et al., 2017), which provides contrail quantities and properties discretized to the aforementioned global grid. More information on CERM can be found in Section 2.2.1. Maximum contrail overlap assumes that all contrails in a single vertical grid column overlap to the greatest possible extent by area. This estimate includes contrails which are diffuse and/or "sub-visible" (optical depth < 0.03).

Under an upper-bound assumption for the total area of contrail overlaps, we find that 15% of all modeled contrail area overlaps with other contrails at different altitudes. If the effect of cloud-contrail overlap is ignored, the maximum contrail-contrail overlap results in a more than three times increase in the contrail-attributable net radiative forcing. This is made up of a 21% reduction in longwave warming but a 38% decrease in shortwave cooling. However, if cloud-contrail overlap is accounted for, the net impact of contrail-contrail overlap is instead a 3.0% reduction in net contrail-attributable RF. The reduction in longwave warming is 2.0%, exceeding the 1.8% reduction in shortwave forcing. This difference is due to the strong mitigation of shortwave forcing (approximately 1/3 of that under clear sky conditions) by existing clouds, and is consistent with the global sensitivity to contrail-contrail overlaps demonstrated in Section 4.2. The majority of contrail-contrail overlap occurs in low-albedo areas such as the North-Atlantic corridor (area 1) or at high latitudes (areas 3 and 4), resulting in a small absolute effect on net RF (-0.3 mW/m^2).

These results are sensitive to the assumptions regarding the degree of overlap in each model column. We assume that all contrails in a given model column overlap to the maximum extent, providing an upper bound for the total effect of contrail overlap. If we instead assume minimum overlap – where each contrail in the column "avoids" overlap until there is no remaining uncovered area – then contrail-contrail overlap only occurs for 2% of all modeled contrail area. This limitation is explored further in Section 5.

4.3.3 Overall impact of cloud-contrail and contrail-contrail overlap on global RF

Table 5. Contrail global average radiative forcing (daytime value) in mW/m^2 under each set of assumptions (IC: independent contrails; clear-sky OC: overlapping contrails clear-sky; IA: independent contrails all-sky; OA: overlapping contrails all-sky).

	IC	OC	IA	OA
RF_{LW}	+33.3	+32.6	+21.0	+20.6
RF_{SW}	-33.1	-31.9	-11.0	-10.8
Net RF	+0.2	+0.7	+10.0	**+9.7**

Table 5 shows the total contrail-attributable RF with and without clouds, and either accounting for or neglecting the effects of contrail-contrail overlap. We find that contrails induce a net RF of 9.7 mW/m^2

for 2015. This result includes a 3% reduction in overall RF from contrail-contrail overlap, but most of it (93%) is due to overlap with clouds.

Assuming that these impacts are an upper bound, these results suggest that the impacts of cloud-contrail overlap are significant, but that contrail-contrail overlap can likely be neglected in modeling studies under current conditions. However, our result of +9.7 mW/m^2 for the net impact of contrails is at the low end of existing literature estimates (see Table 1). This is due to uncertainties in contrail coverage, contrail optical depth, and contrail optical properties. The global CERM simulation output has an average optical depth per contrail of 0.065 and a global coverage of 0.39% by area, both of which are at the lower end of literature estimates (see Table 1). As a sensitivity test, if we increase the optical depth of all contrails from the CERM output data by a factor of four to give the same average per-contrail optical depth as Schumann et al. (2013), which found a net RF of 49.2 mW/m^2, we find a global net contrail RF of 32.6 mW/m^2. Under these conditions, we find that contrail-contrail overlaps decrease the simulated global RF by 8%.

5 Limitations

5.1 Radiative transfer model

Our radiative forcing model is based on an existing, single layer cloud model (Corti and Peter, 2009). This model has some limitations.

When calculating the total outgoing longwave radiation for each layer, the model includes an estimate of absorption by atmospheric CO_2 and water vapor. Estimates for multiple overlapping layers may therefore double-count this contribution. Additionally, cloud emissivity is estimated as only a function of the cloud optical depth. These limitations may partially explain some of the differences in the calculated outgoing longwave radiative forcing between this model and the Fu-Liou radiative transfer model, as discussed in Section 4.1.4.

The longwave radiative forcing model also assumes all layers to be in equilibrium, and does not account for local temperature feedbacks due to the presence of artificial cloud layers. Finally, we do not account for 3-D effects. Cloud layers are assumed to be vertically homogeneous and edge effects are ignored, as in the reference model. A previous investigation of contrail radiative forcing found that 3-D effects could change simulated radiative forcing by ~10% (Gounou and Hogan, 2007).

Regarding shortwave radiative forcing, we do not account for inhomogeneity in the above-cloud atmospheric transmittance of shortwave radiation, instead considering it to be constant at 73%. Shortwave radiative interactions between contrails and other constituents (such as tropospheric aerosols and water vapor) are also not explicitly accounted for. Secondly, the adapted model uses a two-stream approximation of radiative transfer (Coakley and Chylek, 1975). This has been shown to give accurate results at optical depths below ~1 and solar zenith angles below 75°. However, this results in inaccuracy outside of this range, as shown by comparison to other models (Appendix A). It is difficult to provide a quantitative estimate of the effect that such errors, including the weaker dependence of our model's calculated RF and overlap impacts on solar zenith angle when compared to the FL96 model, might have on the overall results. However, we find that our model estimates a smaller RF than the FL96 model at low solar zenith angles. Annually, the solar zenith angle is between 75 and 90° for 16% of the time globally, and 14.5% of the time at latitudes covering the majority of current commercial flights (30°N - 60°N). This may therefore result in an underestimate of overall contrail-attributable RF by our model.

The two-stream approximation used in this model is most accurate for low optical depths. This is appropriate for contrails and thin natural cirrus, but lower-altitude natural clouds can be much thicker. For this reason, we use an asymmetry parameter for high altitude clouds and contrails based on direct observations (Sanz-Morère et al., 2020), while using an asymmetry parameter similar to that suggested by Corti and Peter (2019) for low altitude clouds.

An additional concern is discussed by Rap et al. (2010). They showed that a correlation exists between the existence of contrails and natural clouds. This could result in bias when the method used to simulate

or estimate natural cloud cover is not consistent with that used for contrail estimation. This is a difficult issue to address for a Lagrangian approach such as ours, and may result in an unquantified bias in our estimated contrail-attributable radiative forcing. Future research using the model presented here may therefore wish to perform additional model validation or calibration to ensure that colocation of contrails and natural clouds is correctly captured.

5.2 Input data

Due to the lack of additional input information, and to provide a conservative estimate, we assume that all contrails overlap maximally within a column. This assumption would not be necessary if additional information was supplied by the base contrail model. For instance, the Lagrangian mentioned model CoCiP (Schumann et al., 2012) includes additional information on contrail location and orientiation that could be used to improve overlap modeling. Currently, we instead assume maximum possible overlap. This provides an upper bound on the impact of multiple cloud layers overlap on contrail RF, important given that we find only a small effect due to contrail-contrail overlap. However a more accurate assessment would be possible using the aforementioned orientation data.

Additionally, contrail coverage could be constrained or calibrated by satellite measurements. Some studies (Kärcher 2009; Iwabuchi et al., 2012) have combined satellite imagery (e.g. from MODIS) with observed cloud coverage data in order to provide an improved estimate of contrail coverage. The combination of these data with single-contrail modeling tools (such as CERM) may help to improve the accuracy of estimated contrail coverage. However, there remain significant uncertainties due to the non-detection of very thin contrails (Kärcher et al., 2009), as well as the difficulty of distinguishing between long-lived contrails and natural cirrus clouds in observational data.

Finally, the natural cloud data provided by CERES is coarsely resolved with only four layers in the vertical dimension, averages every three hours, and lacking some additional useful information. The vertical resolution of CERES is also a challenge. Hogan and Illingworth (2006) found that (for cloud

layers more than 4 km apart) overlap is essentially random, but this information is difficult to incorporate given the low vertical resolution of the CERES product. Alternatives to CERES like CALIPSO or CloudSat (Iwabuchi et al., 2012; Tesche et al., 2016) may provide a useful alternative, as they include both more precise estimates of cloud altitude and additional optical properties of the cloud layers.

These results are also sensitive to the optical depth of the simulated layers. Contrails simulated by CERM have a mean contrail optical depth of 0.065, at the lower end of a significant uncertainty range based on existing literature (see Table 1). Since the effects of overlap increase non-linearly with optical depth, estimates based on models which predict thicker contrails may find a significantly greater impact of overlap. Finally, there remain significant uncertainties in contrail coverage. The usage of reanalysis data (from GEOS-FP) as a meteorological data source has been found to overestimate humidity (Jiang et al., 2015; Davis et al., 2017), likely resulting in an overestimate in contrail coverage and lifetime. Improved estimates of contrail lifetime and formation frequency could significantly affect the frequency, and therefore total impact on contrail-related RF, of cloud-contrail and contrail-contrail overlap.

5.3 Priorities for future work

In light of the limitations outlined above, there are some future research directions which could significantly improve the accuracy of the results from this approach.

Firstly, a more detailed dataset of contrail coverage, including continuous information on contrail position and orientation, would remove the need to assume maximum overlap with natural clouds.

Secondly, multiple improvements can be made with regards to the simulation of natural clouds. Finer vertical resolution would enable better representation of both natural and artificial cloud overlap. Our results are also sensitive to the properties prescribed for natural clouds. Incorporation of natural cloud datasets which estimate or infer cloud properties on a case-by-case basis would be useful in providing a more accurate estimate of the effects of multi-layer overlap.

Finally, the radiative forcing model used here does not account for 3-D effects. A more accurate estimate of overlap impacts, in particular those associated with contrail-contrail overlap, would benefit from incorporating these details into their calculations. This is especially true for shortwave interactions.

6 Conclusions

We develop and apply a radiative transfer model to estimate the effect of cloud-contrail and contrail-contrail overlap on the net radiative forcing from contrails. The results will improve our understanding of the factors which contribute to global contrail RF, and help to improve estimates of current and future contrail RF.

We find that overlap between contrails and natural cloud layers can cause a non-linearity in the net radiative forcing. In most cases, overlap between a contrail and a second cloud layer reduces both the cooling (negative shortwave RF) and warming (positive longwave RF) effects of the contrail. This effect is sensitive to the optical depth of each cloud layer. We find a net increase in radiative forcing when contrails overlap with thick clouds ($\tau > 0.5$), but a net decrease when contrails overlap with thinner clouds. However, overlap between two contrails is in general beneficial for climate, decreasing the total contrail-attributable RF. The magnitude of this effect is sensitive to local conditions, including surface albedo, solar zenith angle, and surface temperature. Under night-time conditions, overlapping between contrails and any other cloud layer consistently reduces the net contrail RF due to the lack of competing shortwave effects.

The radiative forcing attributable to a contrail layer increases by a factor of three due to the presence of natural clouds on a global mean basis, but this varies by region. Clouds have a greater effect on midlatitude contrail radiative effects than in the tropics due to the general trend of greater thickness and lower altitude, while other parameters like atmospheric composition and incoming solar radiation may also play a role. They also have greater effects over oceanic routes. We find that contrails over the North Atlantic corridor

have, on average, a small cooling effect under clear-sky conditions (-0.07 W/m^2 per unit of optical depth) but cause warming (+0.69 W/m^2 per unit of optical depth) in cloudy conditions. This suggests that avoiding cloud-contrail overlaps in this region could yield climate benefits, although implementing a contrail avoidance strategy is itself a non-trivial task (e.g. Teoh et al., 2020). This sensitivity also varies by season, with a 15% decrease in RF per unit of optical depth in the Northern Hemisphere from summer to winter.

For year-2015 atmospheric data and flight activity, we calculate an upper bound for the effect of multiple layer overlap on contrail attributable radiative forcing. We find that the presence of natural clouds reduces global contrail longwave radiative forcing by 37%, and the shortwave radiation reflectance by 66%. This is found to result in a net increase in global contrail-attributable RF. Global contrail net RF potential instead decreases by 3% when accounting for contrail-contrail overlap. However, the magnitude of this effect is dependent on the optical thickness of the contrails, which remains highly uncertain (global estimations of average contrail optical depth can vary from ~0.065 to ~0.3).

Acknowledgments

The GEOS-FP meteorological data used in this study have been provided by the Global Modeling and Assimilation Office (GMAO) at the NASA Goddard Space Flight Center. This work was also partially funded by two separate grants: from the “la Caixa” Foundation through their Full Graduate Fellowship, and through NASA grant NNX14AT22A.

Code and Data availability

The codes and data used to produce this work are available from the authors upon request.

Author contributions

SB, RS, and SDE were responsible for the conceptual design of the study. FA, RS, and SDE provided continuous review of the study progress and direction during execution. ISM performed all model simulations and wrote the manuscript. All authors contributed to manuscript editing.

Competing interests

The authors declare no competing interests.

References

Airbus: Airbus Global Market Forecast 2019-2038. [online] Available from: https://www.airbus.com/aircraft/market/global-market-forecast.html

Baran, A. J.: From the single-scattering properties of ice crystals to climate prediction: A way forward, Atmos. Res., 112, 45–69, doi:10.1016/J.ATMOSRES.2012.04.010, 2012.

Barker, H. W., Kato, S. and Wehr, T.: Computation of Solar Radiative Fluxes by 1D and 3D Methods Using Cloudy Atmospheres Inferred from A-train Satellite Data, Surv. Geophys., 33(3), 657–676, doi:10.1007/s10712-011-9164-9, 2012.

Barker, H. W. (2008), Representing cloud overlap with an effective decorrelation length: An assessment using CloudSat and CALIPSO data, J. Geophys. Res., 113, D24205, doi:10.1029/2008JD010391.

Bedka, S. T., Minnis, P., Duda, D. P., Chee, T. L., and Palikonda, R. (2013), Properties of linear contrails in the Northern Hemisphere derived from 2006 Aqua MODIS observations, *Geophys. Res. Lett.*, 40, 772– 777, doi:10.1029/2012GL054363.

Bock, L., and Burkhardt, U.: Reassessing properties and radiative forcing of contrail cirrus using a climate model, J. Geophys. Res. Atmos., 121, 9717– 9736, doi:10.1002/2016JD025112, 2016.

Bock, L. and Burkhardt, U.: Contrail cirrus radiative forcing for future air traffic, Atmos. Chem. Phys., 19, 8163–8174, https://doi.org/10.5194/acp-19-8163-2019, 2019.

Boeing: Boeing Current Market Outlook 2019-2038. [online] Available from: https://www.boeing.com/resources/boeingdotcom/commercial/market/commercial-market-outlook/assets/downloads/cmo-2019-report-final.pdf.

Burkhardt, U. and Kärcher, B.: Global radiative forcing from contrail cirrus, Nat. Clim. Chang., 1(1), 54–58, doi:10.1038/nclimate1068, 2011.

S. J. Byrnes, “Multilayer optical calculations arXiv : 1603 . 02720v2 [physics . comp-ph] 28 Aug 2016,” pp. 1–20, 2016.

Caiazzo, F., Agarwal, A., Speth, R. L. and Barrett, S. R. H.: Impact of biofuels on contrail warming, Environ. Res. Lett., 12(11), 114013, doi:10.1088/1748-9326/aa893b, 2017.

Chen, C.-C. and Gettelman, A.: Simulated radiative forcing from contrails and contrail cirrus, Atmos. Chem. Phys., 13(24), 12525–12536, doi:10.5194/acp-13-12525-2013, 2013.

Coakley, J. A., and P. Chylek, 1975: The two-stream approximation in radiative transfer: Including the angle of the incident radiation. J. Atmos. Sci., 32, 409–418.

Corti, T. and Peter, T.: A simple model for cloud radiative forcing, Atmos. Chem. Phys., 9(15), 5751–5758, doi:10.5194/acp-9-5751-2009, 2009.

Davis, A. B. and Marshak, A.: Solar radiation transport in the cloudy atmosphere: a 3D perspective on observations and climate impacts, Reports Prog. Phys., 73(2), 026801, doi:10.1088/0034-4885/73/2/026801, 2010.

Davis, S. M., Hegglin, M. I., Fujiwara, M., Dragani, R., Harada, Y., Kobayashi, C., Long, C., Manney, G. L., Nash, E. R., Potter, G. L., Tegtmeier, S., Wang, T., Wargan, K., and Wright, J. S.: Assessment of upper tropospheric and stratospheric water vapor and ozone in reanalyses as part of S-RIP, Atmos. Chem. Phys., 17, 12743–12778, https://doi.org/10.5194/acp-17-12743-2017, 2017.

Dessler, A. E. and Yang, P.: The Distribution of Tropical Thin Cirrus Clouds Inferred from Terra MODIS Data, J. Clim., 16(8), 1241–1247, doi:10.1175/1520-0442(2003)16<1241:TDOTTC>2.0.CO;2, 2003.

Febvre, G., Gayet, J.-F., Minikin, A., Schlager, H., Shcherbakov, V., Jourdan, O., Busen, R., Fiebig, M., Kärcher, B. and Schumann, U.: On optical and microphysical characteristics of contrails and cirrus, J. Geophys. Res. Atmos., 114(D2), doi:10.1029/2008JD010184, 2009.

Frömming, C., Ponater, M., Burkhardt, U., Stenke, A., Pechtl, S. and Sausen, R.: Sensitivity of contrail coverage and contrail radiative forcing to selected key parameters, Atmos. Environ., 45(7), 1483–1490, doi:10.1016/J.ATMOSENV.2010.11.033, 2011.

Fu, Q. and Liou, K. N.: Parameterization of the Radiative Properties of Cirrus Clouds, J. Atmos. Sci., 50(13), 2008–2025, doi:10.1175/1520-0469(1993)050<2008:POTRPO>2.0.CO;2, 1993.

Fu, Q. A.: An accurate parameterization of the solar radiative properties of cirrus clouds for climate models, J. Clim., 9, 2058–2082,1996

Fu, Q., Liou, K. N., Cribb, M., Charlock, T. P., and Grossman, A.: Multiple scattering parameterization in thermal infrared radiative transfer, J. Atmos. Sci., 54, 2799–2812, https://doi.org/10.1175/1520-0469(1997)054<2799:MSPITI>2.0.CO;2, 1997.

Gayet, J.-F., Shcherbakov, V., Voigt, C., Schumann, U., Schäuble, D., Jessberger, P., Petzold, A., Minikin, A., Schlager, H., Dubovik, O., and Lapyonok, T.: The evolution of microphysical and optical properties of an A380 contrail in the vortex phase, Atmos. Chem. Phys., 12, 6629-6643, https://doi.org/10.5194/acp-12-6629-2012, 2012.

Geleyn, J. F., and A. Hollingsworth, 1978: An economical analytical method for the computation of the interaction between scattering and line absorption of radiation. Beitr. Phys. Atmos., 52, 1–16.

Gerber, H., Y. Takano, T. J. Garrett, and P. V. Hobbs (2000), Nephelometermeasurements of the asymmetry parameter, volume extinction coefficient,and backscatter ratio in Arctic clouds,J. Atmos. Sci.,57, 3021–3034.

Gounou, A., and R. J. Hogan, 2007: A sensitivity study of the effect of horizontal photon transport on the radiative forcing of contrails. J. Atmos. Sci., 64, 1706–1716.

Hanrahan, Pat and Krüger Wolfgang. “Reflection from layered surfaces due to subsurface scattering.” SIGGRAPH '93 (1993).

Heymsfield, A. J. and Platt, C. M. R.: A Parameterization of theParticle-Size Spectrum of Ice Clouds in Terms of the Ambient-Temperature and the Ice Water-Content, J. Atmos. Sci., 41, 846–855, 1984

Heymsfield, A. J.; Lawson, R. P.; Sachse, G. W. Growth of ice crystals in a precipitating contrail. Geophys. Res. Lett. 1998, 25, 1335– 1338, doi:10.1029/98GL00189

Heymsfield, A., Winker, D., Avery, M., Vaughan, M., Diskin, G., Deng, M., Mitev, V., and Matthey, R.: Relationsips between ice water content and volume extinction coefficient from in situ observations for temperatures from 0◦ to −86◦C: Implications for spaceborne lidar retrievals, J. Appl. Meteorol. Clim., 53, 479–505, 2014.

Hogan, R.J. and Illingworth, A.J. (2000), Deriving cloud overlap statistics from radar. Q.J.R. Meteorol. Soc., 126: 2903-2909. doi:10.1002/qj.49712656914

Hogan, R. J., Shonk, J. K. P.: Incorporating the Effects of 3D Radiative Transfer in the Presence of Clouds into Two-Stream Multilayer Radiation Schemes, J. Atmos. Sci., 70(2), 708–724, doi:10.1175/JAS-D-12-041.1, 2013.

IPCC 2013 Climate Change: The Physical Science Basis. Contribution of Working Group I to the Fifth Assessment Report of the Intergovernmental Panel on Climate Change (Cambridge and New York: Cambridge University Press), 2013.

Jiang, J. H., Su, H., Zhai, C., Wu, L., Minschwaner, K., Molod, A. M., and Tompkins, A. M. (2015), An assessment of upper troposphere and lower stratosphere water vapor in MERRA, MERRA2, and ECMWF reanalyses using Aura MLS observations, J. Geophys. Res. Atmos., 120, 11,468– 11,485, doi:10.1002/2015JD023752.

Jourdan, O., Oshchepkov, S., Shcherbakov, V., Gayet, J.-F., and Isaka, H. (2003), Assessment of cloud optical parameters in the solar region: Retrievals from airborne measurements of scattering phase functions, J. Geophys. Res., 108, 4572, doi:10.1029/2003JD003493, D18.

Kalogirou, S. A.: Solar energy engineering: processes and systems. Burlington, MA, USA; San Diego, CA, USA; London, UK: Elsevier, Academic Press. Available from: https://www.sciencedirect.com/science/book/9780123972705, 2014.

Kärcher, B.: Properties of subvisible cirrus clouds formed by homogeneous freezing, Atmos. Chem. Phys., 2(2), 161–170, doi:10.5194/acp-2-161-2002, 2002.

Kärcher, B., U. Burkhardt, S. Unterstrasser, and P. Minnis (2009), Factors controlling contrail cirrus optical depth, Atmos. Chem. Phys., 9(16), 6229–6254, doi:10.5194/acp-9-6229-2009.

Kärcher, B.: Formation and radiative forcing of contrail cirrus, Nat. Commun., doi:10.1038/s41467-018-04068-0, 2018.

Kim, Y.-H., S.-K. Min, S.-W. Son, and J. Choi (2017), Attribution of the local Hadley cell widening in the Southern Hemisphere, Geophys. Res. Lett., 44, 1015–1024, doi:10.1002/2016GL072353.

Kokhanovsky, A.: Optical properties of terrestrial clouds, Earth-Science Rev., 64(3–4), 189–241, doi:10.1016/S0012-8252(03)00042-4, 2004.

Lee, D. S., Fahey, D. W., Forster, P. M., Newton, P. J., Wit, R. C. N., Lim, L. L., Owen, B. and Sausen, R.: Aviation and global climate change in the 21st century, Atmos. Environ., 43(22–23), 3520–3537, doi:10.1016/J.ATMOSENV.2009.04.024, 2009.

Liou, K.-N.: Influence of Cirrus Clouds on Weather and Climate Processes: A Global Perspective, Mon. Weather Rev., 114(6), 1167–1199, doi:10.1175/1520-0493(1986)114<1167:IOCCOW>2.0.CO;2, 1986.

Liou, K. N., Yang, P., Takano, Y., Sassen, K., Charlock, T. and Arnott, W.: On the radiative properties of contrail cirrus, Geophys. Res. Lett., doi:10.1029/97GL03508, 1998.

Loeb, N. G., Doelling, D. R., Wang, H., Su, W., Nguyen, C., Corbett, J. G., Liang, L., Mitrescu, C., Rose, F. G. and Kato, S.: Clouds and the Earth's Radiant Energy System (CERES) Energy Balanced and Filled (EBAF) Top-of-Atmosphere (TOA) Edition-4.0 Data Product, J. Clim., 31(2), 895–918, doi:10.1175/JCLI-D-17-0208.1, 2018.

Lolli, S., Campbell, J. R., Lewis, J. R., Gu, Y. and Welton, E. J.: Technical note: Fu–Liou–Gu and Corti–Peter model performance evaluation for radiative retrievals from cirrus clouds, Atmos. Chem. Phys., 17(11), 7025–7034, doi:10.5194/acp-17-7025-2017, 2017.

Marchand, R., Ackerman, T., Smyth, M., and Rossow, W. B. (2010), A review of cloud top height and optical depth histograms from MISR, ISCCP, and MODIS, J. Geophys. Res., 115, D16206, doi:10.1029/2009JD013422.

Markowicz, K. M., and M. L. Witek, 2011a: Simulations of Contrail Optical Properties and Radiative Forcing for Various Crystal Shapes. *J. Appl. Meteor. Climatol.*, **50**, 1740–1755, https://doi.org/10.1175/2011JAMC2618.1.

Markowicz, K. M., and Witek, M. (2011b), Sensitivity study of global contrail radiative forcing due to particle shape, *J. Geophys. Res.*, 116, D23203, doi:10.1029/2011JD016345.

Marquart, S., Ponater, M., Mager, F. and Sausen, R.: Future Development of Contrail Cover, Optical Depth, and Radiative Forcing: Impacts of Increasing Air Traffic and Climate Change, J. Clim., 16(17), 2890–2904, doi:10.1175/1520-0442(2003)016<2890:FDOCCO>2.0.CO;2, 2003.

Meerkötter, R., Schumann, U., Doelling, D. R., Minnis, P., Nakajima, T. and Tsushima, Y.: Radiative forcing by contrails, Ann. Geophys., 17(8), 1080–1094, doi:10.1007/s00585-999-1080-7, 1999.

Minnis, P., Schumann, U., Doelling, D. R., Gierens, K. M. and Fahey, D W..: Global distribution of contrail radiative forcing, Geophys. Res. Lett., 26(13), 1853–1856, doi:10.1029/1999GL900358, 1999.

Minnis, Patrick & Trepte, Qing & Sun-Mack, Sunny & Chen, Yan & Doelling, David & Young, David & Spangenberg, Douglas & Miller, Walter & Wielicki, Bruce & Brown, Ricky & Gibson, Sharon & Geier, Erika. (2008). Cloud detection in nonpolar regions for CERES using TRMM VIRS and terra and aqua MODIS data. Geoscience and Remote Sensing, IEEE Transactions on. 46. 3857 - 3884. 10.1109/TGRS.2008.2001351.

Minnis P., et al., 2013: Linear contrail and contrail cirrus properties determined from satellite data, Geophys. Res. Lett., 40, 3220-3226.

Myhre, G., Kvalevåg, M., Rädel, G., Cook, J., Shine, K. P., Clark, H., Kärcher, F., Markowicz, K., Kardas, A., Wolkenberg, P., Balkanski, Y., Ponater, M., Forster, P., Rap, A., Leon, R. and Rodriguez: Intercomparison of radiative forcing calculations of stratospheric water vapour and contrails, Meteorol. Zeitschrift, 18(6), 585–596, doi:10.1127/0941-2948/2009/0411, 2009.

NASA Langley Research Center Atmospheric Science Data Center 2015 CERES SYN1deg Observed Radiative Fluxes and Clouds with Computed Profile Fluxes (https://ceres-tool.larc.nasa.gov/ord-tool/jsp/SYN1degEd4Selection.jsp)

National Oceanic and Atmospheric Administration Earth System Research Laboratory 2015 Rapid Refresh (http://rapidrefresh. noaa.gov/)

Nousiainen, T. and McFarquhar, G. M.: Light Scattering by Quasi-Spherical Ice Crystals, J. Atmos. Sci., 61(18), 2229–2248, doi:10.1175/1520-0469(2004)061<2229:LSBQIC>2.0.CO;2, 2004.

Norris, J. R., Allen, R. J., Evan, A. T., Zelinka, M. D., O'Dell, C. W. and Klein, S. A.: Evidence for climate change in the satellite cloud record, Nature, 536, 72 [online] Available from: https://doi.org/10.1038/nature18273, 2016.

Olsen, S. C., Wuebbles, D. J., and Owen, B.: Comparison of global 3-D aviation emissions datasets, Atmos. Chem. Phys., 13, 429-441, https://doi.org/10.5194/acp-13-429-2013, 2013.

Penner, J. E., D. H. Lister, D. J. Griggs, D. J. Dokken, and M. McFarland, 1999: Aviation and the Global Atmosphere – A Special Report of IPCC Working Groups I and III. Intergovernmental Panel on Climate

Change. Cambridge University Press, https://www.ipcc.ch/report/aviation-and-the95 global-atmosphere-2/, 365 pp.

Ponater, M., Marquart, S. and Sausen, R.: Contrails in a comprehensive global climate model: Parameterization and radiative forcing results, J. Geophys. Res. Atmos., 107(D13), ACL 2-1-ACL 2-15, doi:10.1029/2001JD000429, 2002.

Radel, G. and Shine, K. P.: Radiative forcing by persistent contrails and its dependence on cruise altitudes, J. Geophys. Res. Atmos., 113(D7), doi:10.1029/2007JD009117, 2008.

Rap, A., Forster, P. M., Jones, A., Boucher, O., Haywood, J. M., Bellouin, N., and De Leon, R. R. (2010), Parameterization of contrails in the UK Met Office Climate Model, J. Geophys. Res., 115, D10205, doi:10.1029/2009JD012443.

Roeckner,E., Arpe,K., Bengtsson,L., Christoph,M., Claussen,M., Dümenil,L., Esch,M., Giorgetta,M., Schlese,U. and Schulzweida,U. 1996 The atmospheric general circulation model ECHAM-4: model description and simulation of present-day climate Max-Planck Institute for Meteorology, Report No.218, Hamburg, Germany, 90pp.

Sanz-Morère, I., Eastham, S. D., Speth, R. L. and Barrett, S. R. H. (2020): Reducing Uncertainty in Contrail Radiative Forcing Resulting from Uncertainty in Ice Crystal Properties, Environ. Sci. Technol. Lett., 0(0), null, doi:10.1021/acs.estlett.0c00150, n.d.

Sassen, K., Wang, Z., and Liu, D. (2008), Global distribution of cirrus clouds from CloudSat/Cloud-Aerosol Lidar and Infrared Pathfinder Satellite Observations (CALIPSO) measurements, J. Geophys. Res.,113, D00A12, doi:10.1029/2008JD009972

Schumann, U.: Influence of propulsion efficiency on contrail formation, Aerosp. Sci. Technol., 4(6), 391–401, doi:10.1016/S1270-9638(00)01062-2, 2000.

Schumann, U., Mayer, B., Gierens, K., Unterstrasser, S., Jessberger, P., Petzold, A., Voigt, C. and Gayet, J.-F.: Effective Radius of Ice Particles in Cirrus and Contrails, J. Atmos. Sci., 68(2), 300–321, doi:10.1175/2010JAS3562.1, 2011.

Schumann, U.: A contrail cirrus prediction model, Geosci. Model Dev., 5(3), 543–580, doi:10.5194/gmd-5-543-2012, 2012.

Schumann, U., Mayer, B., Graf, K. and Mannstein, H.: A Parametric Radiative Forcing Model for Contrail Cirrus, J. Appl. Meteorol. Climatol., 51(7), 1391–1406, doi:10.1175/JAMC-D-11-0242.1, 2012.

Schumann, U. and Graf, K.: Aviation-induced cirrus and radiation changes at diurnal timescales, J. Geophys. Res., 118, 2404–2421, doi:10.1002/jgrd.50184, 2013.

Schumann, U., Penner, J. E., Chen, Y., Zhou, C. and Graf, K.: Dehydration effects from contrails in a coupled contrail–climate model, Atmos. Chem. Phys., 15(19), 11179–11199, doi:10.5194/acp-15-11179-2015, 2015.

Schumann, U., Baumann, R., Baumgardner, D., Bedka, S. T., Duda, D. P., Freudenthaler, V., Gayet, J.-F., Heymsfield, A. J., Minnis, P., Quante, M., Raschke, E., Schlager, H., Vázquez-Navarro, M., Voigt, C. and Wang, Z.: Properties of individual contrails: a compilation of observations and some comparisons, Atmos. Chem. Phys., 17(1), 403–438, doi:10.5194/acp-17-403-2017, 2017.

Schumann, U. and Heymsfield, A. J.: On the Life Cycle of Individual Contrails and Contrail Cirrus, Meteorol. Monogr., 58, 3.1-3.24, doi:10.1175/AMSMONOGRAPHS-D-16-0005.1, 2017.

Schwarz, M., Folini, D., Yang, S. et al. Changes in atmospheric shortwave absorption as important driver of dimming and brightening. Nat. Geosci. 13, 110–115 (2020). https://doi.org/10.1038/s41561-019-0528-y

Simone, N.W., Stettler, M.E.J., Barrett, S.R.H., 2013. Rapid estimation of global civil aviation emissions with uncertainty quantification. Transp. Res. Part D Transp. Environ. 25, 33–41. https://doi.org/10.1016/j.trd.2013.07.001

Spangenberg, D.A., Minnis, P., Bedka, S.T., Palikonda, R., Duda, D.P., Rose, F.G., 2013. Contrail radiative forcing over the Northern Hemisphere from 2006 Aqua MODIS data. Geophys. Res. Lett. 40, 595–600. https://doi.org/10.1002/grl.50168

Stephens, G. L., Tsay, S. C., Stackhouse, P. W., and Flatau, P. J.: The Relevance of the Microphysical and Radiative Properties of Cirrus Clouds to Climate and Climatic Feedback, J. Atmos. Sci., 47, 1742–1753, 1990.

Tesche, M., Achtert, P., Glantz, P. et al. Aviation effects on already-existing cirrus clouds. Nat Commun 7, 12016 (2016). https://doi.org/10.1038/ncomms12016

Teoh, R., Schumann, U., Majumdar, A., Stettler, M.E.J., 2020. Mitigating the Climate Forcing of Aircraft Contrails by Small-Scale Diversions and Technology Adoption. Environ. Sci. Technol. 54, 2941–2950. https://doi.org/10.1021/acs.est.9b05608

Warren, S. G., C. H. Hahn, J. London, R. M. Chervin, and R. L. Jenne, 1988: Global Distribution of Total Cloud Cover and Cloud Type Amounts Over the Ocean. NCAR Technical Note NCAR/TN-317+STR, doi:10.5065/D6QC01D1.

Wilkerson, J.T., Jacobson, M.Z., Malwitz, A., Balasubramanian, S., Wayson, R., Fleming, G., Naiman, A.D., and Lele, S.K. (2010). Analysis of emission data from global commercial aviation: 2004 and 2006. Atmos. Chem. Phys. Discuss. 10, 2945-2983.

Yang, P., Baum, B. A., Heymsfield, A. J., Hu, Y. X., Huang, H.-L., Tsay, S.-C. and Ackerman, S.: Single-scattering properties of droxtals, J. Quant. Spectrosc. Radiat. Transf., 79–80, 1159–1169, doi:10.1016/S0022-4073(02)00347-3, 2003.

Appendix A: Radiative forcing model validation

To validate the results of our model, we test the simulated radiative forcing for a single contrail layer against the existing FL96 (Fu and Liou, 1993; Fu, 1996) and CoCiP (Schumann, 2012) cirrus cloud radiative transfer models. Section A1 describes the different inputs for the three models, and demonstrates how the RF simulated by each model varies as a function of the chosen input parameters. In Section A2, we simulate the change in shortwave RF as a function of surface albedo in all three models. We then simulate the effect of overlap on both components using our model and FL96 is included in the paper in Section 3.1.4. In the comparison case we obtain, for RF_{SW}, a difference of less than 15% for $\theta < 80^{o}$ (with smaller difference at smaller solar zenith angles), while at high solar zenith angles ($\theta > 80^{o}$), this difference can grow to up to 20%, while the difference in RF_{LW} is always within 10%.

A1 Validation of our model against existing approaches

Each of the three models uses a different representation of ice particle optical properties. FL96 uses a "generalized diameter", assuming hexagonal ice columns (Fu and Liou, 1993). CoCiP can simulate a number of different ice particle shapes, but requires an effective radius. Our model requires instead the asymmetry parameter of the layer. To enable reasonable comparisons, we start from the most complex of the three models, FL96. This represents the ice crystals using a "generalized diameter" that we choose between 20 and 130 μm. We use data from table 1 of Fu (1996) to deduce the effective radius used for CoCiP (21-112 μm). We finally use Fig. 5 from Key et al. (2002) to estimate the asymmetry parameter corresponding to each given particle radius (0.75 – 0.92).

To test the level of agreement, we simulate a single contrail layer under clear-sky conditions. We use a fixed contrail altitude (11 km), a fixed albedo of 0.3, and a fixed outgoing longwave radiation flux of 278 W/m^2, with no aerosol layers. We simulate multiple optical depths between 0.01 and 0.5, and simulate the effect for solar zenith angles of 0 to 90°. Figure A1 shows the RF components simulated by each model when sweeping across the given range of optical properties. The positive values are the longwave component, while the negative values are the shortwave.

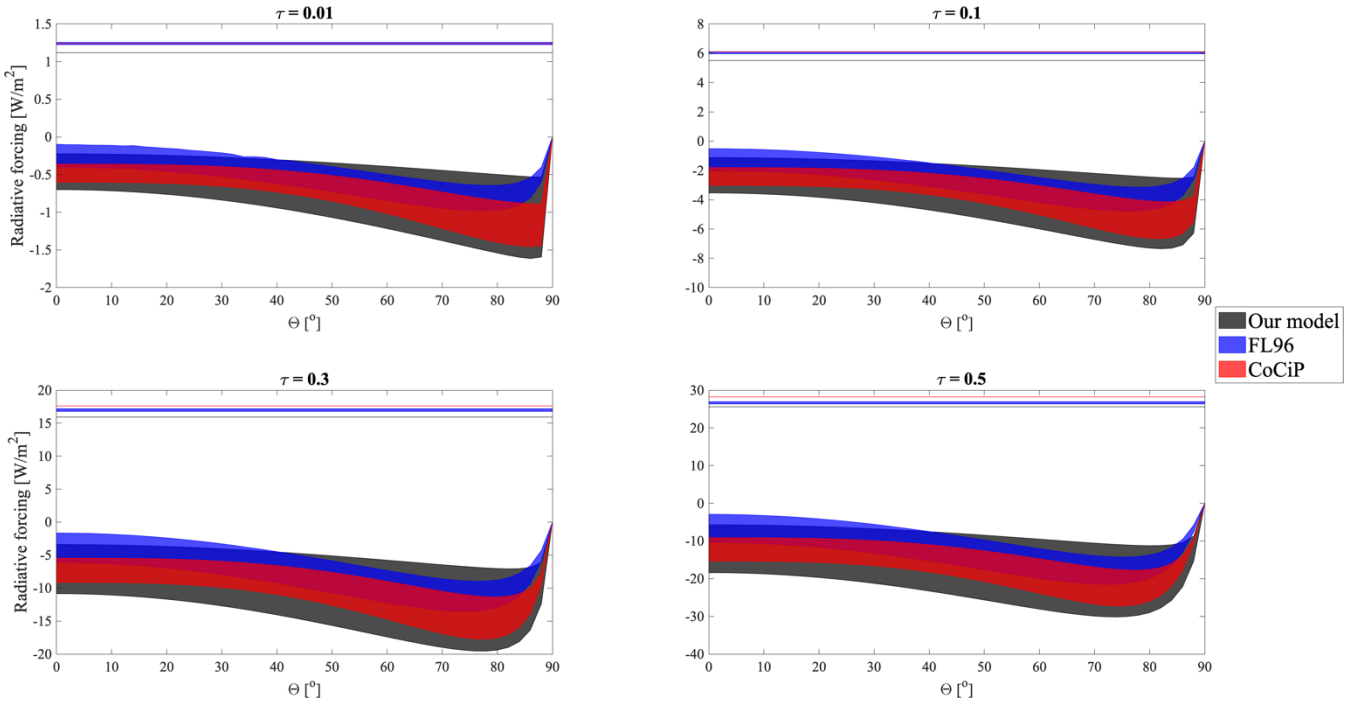

Figure A1: Longwave (positive) and shortwave (negative) radiative forcing ranges (varying particle size) in W/m^2 with the three models tested here: our model (based on Corti and Peter), FL96, and CoCiP. Variations with optical depth and solar zenith angle are shown.

Qualitatively, the models behave similarly. Variation in longwave radiative forcing in response to changing optical properties is negligible in all three models, but our model consistently estimates a lower RF_{LW} than is estimated by CoCiP. This error is maximized at low optical depths, reaching ~10%. The estimate from FL96 varies, agreeing more closely with CoCiP at low optical depths and more closely with our model at high optical depths.

Shortwave radiative forcing varies significantly with changes in optical properties in all three models. The range of asymmetry parameters simulated by our model results in a greater overall variation than is observed in the range of properties tested for FL96 or CoCiP. Qualitatively, the behavior of our model as the solar zenith angle (θ) increases matches that of CoCiP closely. RF_{SW} increases slowly with θ, before

reaching a peak between θ = 75° (high optical depths) and 88° (low optical depths). At values of θ beyond this peak, RF_{SW} falls rapidly to 0. In FL96, the shape of the relationship is similar at all optical depths, with the minimum value occurring approximately at 75°. We also evaluate the difference in average value for each of the models, within the ranges of comparable microphysical properties. We obtain an average difference of less than 10% between CoCiP and our model, with the greatest error being ~20% at θ > 80°, expected from the here used two-stream approximation and mentioned in the limitations section. We find a greater average difference of ~40% between our model and FL96.

To perform more quantitative analysis and comparison, we select a specific value of the relevant optical parameter for each model. For this purpose we choose an effective radius for ice of 45 μm. This is consistent with a natural ice cloud at an altitude of ~11 km, based on published parameterizations (Heymsfield and Platt, 1984; Corti and Peter, 2009; Lolli et al, 2017; Heymsfield, 2014). A prior analysis by Corti and Peter (2009) found that an asymmetry parameter *g* of 0.87 gave results which most closely matched those from FL96, and as such we use that value here. Key et al. (2002) also confirmed that this is consistent with solid columns of the mentioned size. Using the approach outlined earlier, this crystal size is represented in CoCiP using an effective radius of 45 μm and in FL96 using a generalized diameter of 46 μm. This specific single-contrail experiment results in differences in RF_{SW} between our model and FL96 which are below 15%.

A2 Comparison of albedo effect on single contrail RF_{SW}

To evaluate the accuracy of our single contrail radiative forcing model, we simulate the effect of changes in surface albedo on single contrail shortwave radiative forcing and compare the results to both FL96 and CoCiP. Figure A2 shows the variation of RF_{SW} with albedo in each model at three different optical depths. As previously explained, CoCiP uses an effective radius of 45 μm and FL96 uses a generalized diameter of 46 μm, while our model is using an asymmetry parameter of $g = 0.87$.

We observe the same qualitative behavior in all 3 models. Neglecting the already mentioned differences at high solar zenith angles (θ > 80°), FL96 and CoCiP quantitatively agree best with our model at low

albedos ($\alpha < 0.5$), with overall differences below 30%. Our model predicts a higher cooling impact at low solar zenith angles, and a lower cooling at high solar zenith angles. Maximum differences are found at high albedos ($\alpha > 0.6$) and high solar zenith angles ($\theta > 50°$), where our model significantly underestimates RF_{SW}, with differences of approximately 50%. However, these differences are less than 2 W/m^2 in absolute terms. The best agreement is found at an albedo of 0.3, the global Earth average albedo, with less than 10% difference. Finally, there are significant differences with CoCiP at low solar zenith angles and high albedos due to the forced negative sign of RF_{SW} with that model. All percentage differences between the models are insensitive to changes in optical depth.

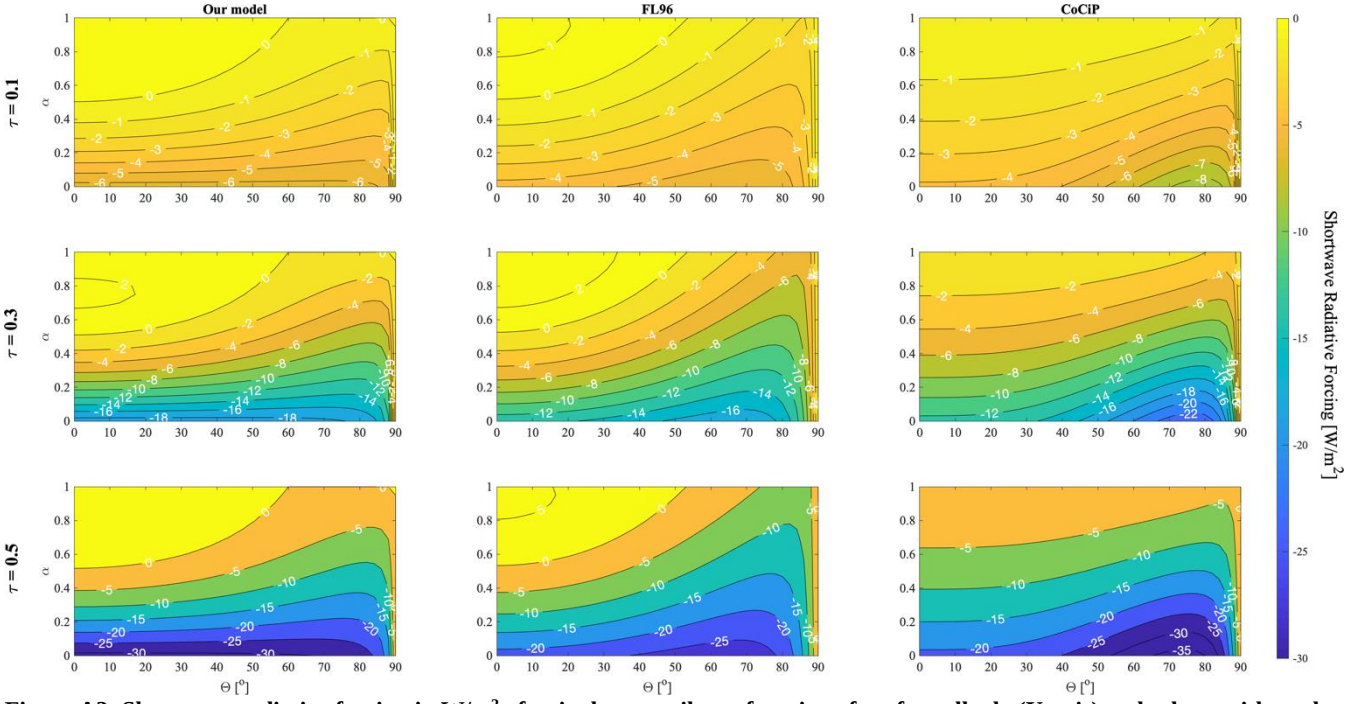

Figure A2: Shortwave radiative forcing in W/m^2 of a single contrail as a function of surface albedo (Y-axis) and solar zenith angle (X-axis). Each column corresponds to a different model, and each row corresponds to a different contrail optical depth.

To highlight these differences, we analyze one specific metric in all three models. Figure A3 shows the ratio of RF_{SW} for an albedo of 0.5 to RF_{SW} for an albedo of 0.3. In FL96, the ratio increases approximately linearly from ~0.1 to ~0.9 as the solar zenith angle increases from 0 to 90°. We also find a small increase in the ratio as a function of optical depth, although this falls with increasing solar zenith angle.

Our model shows similar behavior in response to the change in solar zenith angle, although the increase is from ~0.03 to ~0.70 over the same range. One noticeable difference is the behavior at very high solar zenith angles. The rate of change of the ratio increases sharply in FL96 at a solar zenith angle of ~85°, but in our model no such change is observed. This is consistent with the error resulting from the two-stream approximation (Coakley and Chylek, 1975; Corti and Peter, 2009) and is commented on in the Limitations section. The change in the ratio as a function of optical depth is also qualitatively similar.

By contrast, the ratio in CoCiP is almost constant at ~0.62. However, CoCiP does reproduce the sharp increase at high solar zenith angles that is simulated by FL96.

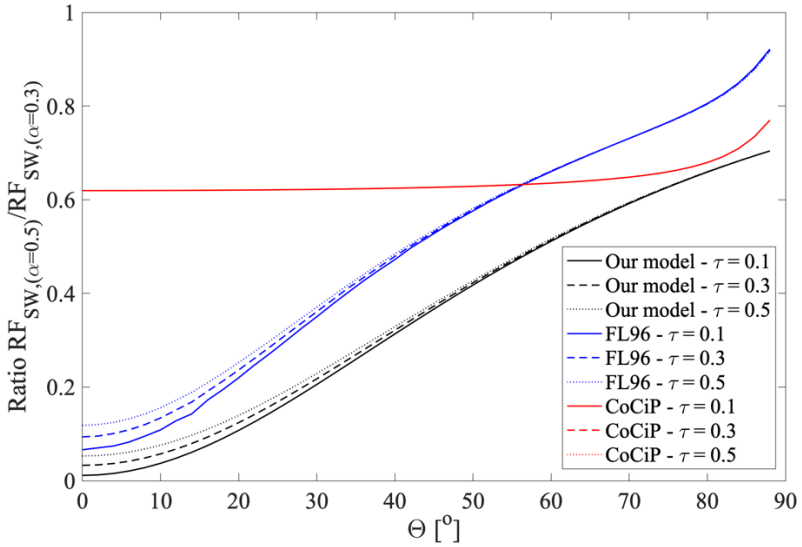

Figure A3: Ratio of shortwave radiative forcing for two different surface albedos as a function of solar zenith. Each color corresponds to a different model, and each line style (continuous, dashed, and dotted) corresponds to a different optical depth.

Appendix B: Shortwave RF model for overlapping layers

B1 Simplification of reflections between two infinite layers

Different formulations have been developed to address radiation transfer between multiple layers, solving problems from very diverse topics: from estimating scattering in layered surfaces, through 1D transport theories (Hanrahan and Krüger, 1993) or by the transport matrix method (Byrnes, 2019), to representing

cloud overlap with an effective decorrelation length (Barker, 2008). The simple expression of reflectance from Coakley and Chylek (1975), used in Corti and Peter model, allows us to develop our own formulation.

In this section we develop the formulation for calculating shortwave radiative forcing for a 2- and 3-layers overlap and deduce a formulation applicable to an N-layers overlap. We start by recalling single contrail RF_{SW} equation (Section B1.1), defined in main paper. We then develop the formulation for a 2-layers overlap (Section B1.2) and finish by extend the formulation to an N-layers overlap (Section B1.3), resulting in a simple formula easily applicable to our contrail coverage data.

B1.1 Single layer RF_{SW}

When evaluating shortwave radiative forcing of *N* infinite overlapping layers, we have to consider all the interactions between layers including reflectance and transmittance. We assume that cloud layers reflect shortwave radiation without diffusing it, whereas the Earth's surface diffuses incoming radiation in every direction (Corti and Peter 2009). Using these assumptions, we can decompose mathematically all the radiation interactions between layers.

As given in Section 2.1.1, the shortwave radiative forcing of a single contrail can be expressed as

$$RF_{SW} = -S \cdot t(1-\alpha)\left(\frac{R-\alpha R'}{1-\alpha R'}\right) \tag{B1}$$

where *S* is the solar constant, α is the Earth's surface albedo, *t* is the mean atmospheric transmittance, and *R* and *R'* are the direct and diffuse reflectances of the contrail. This expression can be rewritten as

$$RF_{SW} = -S \cdot t(\alpha-\alpha_1) = -S \cdot t(\alpha-\alpha_{11}-\alpha_{12}) = -S \cdot t\left(\alpha - R - \alpha\frac{TT'}{1-\alpha R'}\right) \tag{B2}$$

with (*T*, *T'*) being the direct and diffuse transmittances (*T* = 1 - *R*, *T'* = 1 - *R*'). We can divide the shortwave RF of a single contrail (contrail *i*) into two different components, α_{i1} and α_{i2} . The first, α_{i1} is equivalent

to the contrail "albedo" for direct radiation, and is in this case simply R. The second, α_{i2} can then be thought of as the contrail "albedo" for diffuse radiation – in this case, $\alpha \frac{TT'}{1-\alpha R'}$.

B1.2 Two-layer RFsw

Now consider a situation with two overlapping cloud layers, whose optical properties are fully captured by their individual reflectances (R_1 and R_2 for direct, R_1' and R_2' for diffuse). Under the assumptions listed above, and ignoring edge effects, Fig. A1 diagrams the how one incoming unit of radiation (S = 1) will interact with these two layers.

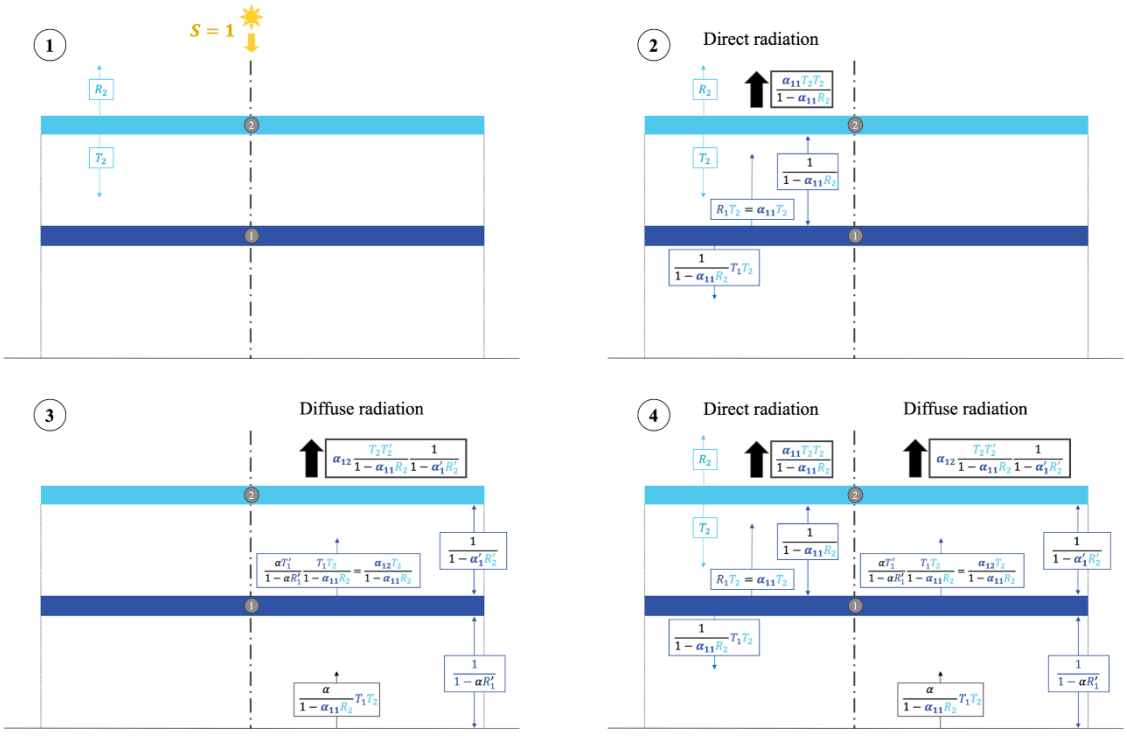

Figure B1. Decomposition of interactions between two cloud layers when receiving a single unit of shortwave radiation (S = 1). Sub-panels 1, 2, and 3 show three successive steps in the calculation as referred to in the text. R_1: direct reflectance, T_1: direct transmission (=1-R_1); R'_1: diffused reflectance, T'_1: diffused transmission (1-R'_1). Subscripts (1 and 2) indicate the layer number. α = Earth albedo. Text color indicates the layer which most recently interacted with the radiation, with radiation from layer 1 in dark blue, from layer 2 in light blue, and from the Earth (reflected) in black.

Subpanel 1 shows the initial interaction between incoming (direct) radiation and the upper contrail (contrail number 2). This contrail reflects a proportion R_2 of the incoming direct light and transmits (allows to pass through) a fraction T_2, equal to 1-R_2. This would show all direct radiation interactions if there were no lower contrail, as light reflecting off the Earth's surface is assumed to be diffuse.

Subpanel 2 shows the full set of interactions for the incoming, direct, radiation when including both contrails. The fraction which passed through the upper contrail, T_2, now undergoes an infinite number of reflections between contrails 1 and 2. On each reflection, some fraction (T_1 and T_2, respectively) of the reflected light passes through. This results in a geometric series, which can be summed to yield the total radiation which passes through the upper contrail (back to space) or lower contrail (towards the ground). Ignoring these reflections, the radiation passing to the ground would be simply T_1T_2; the reflections increase this by a factor of $\frac{1}{1-\alpha_{11}R_2}$, such that $\frac{T_1T_2}{1-\alpha_{11}R_2}$ is the total radiation heading towards the surface. The total which leaves upwards, back to space, is then $R_2 + \frac{\alpha_{11}T_2T_2}{1-\alpha_{11}R_2}$.

Subpanels 3 then shows how diffuse radiation, reflecting off the Earth's surface, interacts with the system. As shown in Subpanel 2, the total direct radiation which reaches the ground is $\left(\frac{\mathrm{T_1T_2}}{1-\alpha_{11}R_2}\right)$, of which only a fraction α is reflected back upwards as diffuse radiation. There are now two sets of infinite reflections to consider. The first is between the Earth and lower contrail, resulting in a geometric series which can be summed to $\frac{1}{1-\alpha\mathrm{R_1'}}$ - now using the diffuse reflectance R_1' instead of the direct reflectance R_1. The second is between the two contrails, and can be expressed using the effective "albedo" of the lower contrail $\alpha_1'(= \alpha_{11}' + \alpha_{12}' = R_1' + R_2')$. This geometric series can then be expressed as $\frac{1}{1-\alpha_1'R_2'}$. From these equations, it becomes clear that the effect of additional contrails is to have additional "albedos", each of which modifies the total radiation which is either reflected to space or eventually absorbed by the Earth's surface (through repeated reflections).

The combination of the direct and diffuse radiation fluxes can then be seen in Subpanel 4; each upwards arrow from contrail 2 represents a separate component which will escape back to space. Adding these together and subtracting from the radiation which would be reflected to space under a clear-sky scenario (i.e. the Earth's albedo), the total shortwave RF can be summarized as

$$RF_{SW} = -S \cdot t(\alpha - \alpha_2) = -S \cdot t(\alpha - \alpha_{21} - \alpha_{22}) = -S \cdot t\left[\alpha - R_2 - \alpha_{11}\frac{T_2 T_2}{1 - R_1 R_2} - \alpha_{12}\left(\frac{T_2 T_2'}{1 - R_1 R_2}\right)\left(\frac{1}{1 - \alpha_1' R_2'}\right)\right] \quad \text{(B3)}$$

where we have now combined the terms into two effective "albedos". These terms allow us to treat the combined layer pair as a if it were a single contrail. Specifically, we have α_{21} $(= R_2 + \alpha_{11}\frac{T_2 T_2}{1 - R_1 R_2})$ being the "albedo" of the layer pair to direct radiation, and α_{22} $(= \alpha_{12}\frac{T_2 T_2'}{1 - R_1 R_2}\frac{1}{1 - \alpha_1' R_2'})$ being the "albedo" of the layer pair to diffuse radiation.

B1.3 *N*-layer RF_{SW}

This approach extends from 2 to *N* layers by following the same mathematical logic (see Table B1), using as "albedo" values (α_i) the direct and diffuse "albedos" of the (N-1) layers below the top one.

Table B1. Developed expression of RF_{SW}/St for multiple layers overlaps

# of layers	RF_{SW} expression $(= -RF_{SW}/St)$
1	$\alpha - \alpha_1 = \alpha - \alpha_{11} - \alpha_{12} = \alpha - R_1 - \frac{T_1}{1 - \alpha R_1'}\alpha T_1'$
2	$\alpha - \alpha_2 = \alpha - \alpha_{21} - \alpha_{22} = \alpha - R_2 - \frac{T_2}{1 - \alpha_{11} R_2}\left(\alpha_{11} T_2 + \frac{\alpha_{12} T_2'}{1 - \alpha_1' R_2'}\right)$
3	$\alpha - \alpha_3 = \alpha - \alpha_{31} - \alpha_{32} = \alpha - R_3 - \frac{T_3}{1 - \alpha_{21} R_3}\left(\alpha_{21} T_3 + \frac{\alpha_{22} T_3'}{1 - \alpha_2' R_3'}\right)$
N	$\alpha - \alpha_N = \alpha - \alpha_{\mathrm{N1}} - \alpha_{\mathrm{N2}} = \alpha - R_N - \frac{T_N}{1 - \alpha_{(\mathrm{N}-1)1} R_N}\left(\alpha_{(\mathrm{N}-1)1} T_N + \frac{\alpha_{(\mathrm{N}-1)2} T_N'}{1 - \alpha_{(N-1)}' R_N'}\right)$

The resulting "albedos" for direct (α_{N1}) and diffuse (α_{N2}) radiation in a N-layer overlap are then the following:

$$\alpha_{\mathrm{N1}} = R_N + \alpha_{(\mathrm{N}-1)1}\frac{T_N T_N}{1-\alpha_{(\mathrm{N}-1)1}R_N} \tag{B4}$$

$$\alpha_{\mathrm{N2}} = \alpha_{(\mathrm{N}-1)2}\frac{T_N T'_N}{1-\alpha_{(\mathrm{N}-1)1}R_N}\cdot\frac{1}{1-\alpha'_{(N-1)}R'_N} \tag{B5}$$

This calculation means that we can collapse the effect of *N* different layers on shortwave radiation into the effect of a single, combined layer, as long as we know the direct and diffuse reflectances of each layer.

If we assume that all layers have the same optical properties (identical asymmetry parameter g and therefore identical optical parameter γ) we can simplify this further. Using the definition of *R* from the main text, we find that the direct albedos for 2 and 3 layers can be written as $\alpha_{21} = \frac{(\tau_1+\tau_2)/\mu}{\gamma+(\tau_1+\tau_2)/\mu}$ and $\alpha_{31} = \frac{(\tau_1+\tau_2+\tau_3)/\mu}{\gamma+(\tau_1+\tau_2+\tau_3)/\mu}$. Extrapolating to an arbitrary *N* layers, we find that

$$\alpha_{\mathrm{N1}} = \frac{\sum_{i=1}^{N}\tau_i/\mu}{\gamma+\sum_{i=1}^{N}\tau_i/\mu} \tag{B6}$$

Therefore, the direct "albedo" from an *N*-layer overlap of similar layers (same optical properties) is equal to the direct reflectance of a single layer with the same total (summed) optical depth. The same logic can be applied to the diffuse albedo.

If the overlap occurs between layers of different optical properties, the same method can be applied as long as a single "effective" asymmetry parameter g_e can be used for all layers. A method to find this parameter is derived below (Section B2). Once this parameter is known, $\mathrm{RF_{SW}}$ for multiple overlapping contrails can be reduced to that for a single layer, i.e.

$$RF_{SW} = -S\cdot t\left(\alpha - R_e - \alpha\frac{T_e T'_e}{1-\alpha R'_e}\right) = -S\cdot t(1-\alpha)\left(\frac{R_e - R'_e}{1-\alpha R'_e}\right) \tag{B7}$$

with $R_e = \frac{\sum_{i=1}^{N} \tau_i/\mu}{\gamma_e + \sum_{i=1}^{N} \tau_i/\mu}$ and $\gamma_e = \frac{1}{1-g_e}$.

B2 Derivation of weighted asymmetry parameter

As outlined above, the calculation of shortwave radiative forcing for an *N*-layer overlap can be simplified significantly if a single, "effective" asymmetry parameter can be identified which characterizes the entire system. To calculate this effective optical parameter, we first determine what would be the effective optical parameter so that the direct radiation "albedos" are equal in both cases. We then show that matching this albedo is sufficient to ensure that the overall radiative forcing (accounting for both diffuse and direct radiation) matches between the "simplified" case and one in which each layer is treated independently.

In an *N*-layer overlap, a proportion α_{N1} of incoming direct radiation is reflected. The single effective layer reflects radiation through the factor R_e. The equality that must hold is then

$$\alpha_{\mathrm{N1}} = R_N + \frac{\alpha_{(\mathrm{N}-1)1} T_N T_N}{1 - \alpha_{(\mathrm{N}-1)1} R_N} = R_e \tag{B9}$$

As for eq. (A6), developing the expression of direct radiation albedo for a 2 and 3-layers overlap we obtain $\alpha_{21} = \frac{\gamma_1\tau_2/\mu + \gamma_2\tau_1/\mu}{\gamma_1\gamma_2 + \gamma_1\tau_2/\mu + \gamma_2\tau_1/\mu}$ and $\alpha_{31} = \frac{\gamma_1\gamma_3\tau_2/\mu + \gamma_2\gamma_3\tau_1/\mu + \gamma_1\gamma_2\tau_3/\mu}{\gamma_1\gamma_2\gamma_3 + \gamma_1\gamma_3\tau_2/\mu + \gamma_2\gamma_3\tau_1/\mu + \gamma_1\gamma_2\tau_3/\mu}$. If we assume that $\alpha_{(\mathrm{N}-1)1} = \frac{\left(\sum_{i=1}^{N-1} \prod_{j\neq i} \gamma_j \tau_i/\mu\right)}{\left(\prod_{i=1}^{N-1} \gamma_i\right) + \left(\sum_{i=1}^{N-1} \prod_{j\neq i} \gamma_j \tau_i/\mu\right)}$, we obtain $\alpha_{\mathrm{N1}} = \frac{\left(\sum_{i=1}^{N} \prod_{j\neq i} \gamma_j \tau_i/\mu\right)}{\left(\prod_{i=1}^{N} \gamma_i\right) + \left(\sum_{i=1}^{N} \prod_{j\neq i} \gamma_j \tau_i/\mu\right)}$. This then yields the following expression, for any N:

$$\alpha_{\mathrm{N1}} = \frac{\left(\sum_{i=1}^{N} \prod_{j\neq i} \gamma_j \, \tau_i/\mu\right)}{\left(\prod_{i=1}^{N} \gamma_i\right) + \left(\sum_{i=1}^{N} \prod_{j\neq i} \gamma_j \, \tau_i/\mu\right)} \tag{B10}$$

Equalizing expression (B10) with the effective reflectance of direct radiation $\left(R_e = \frac{\sum_{i=1}^{N} \tau_i/\mu}{\gamma_e + \sum_{i=1}^{N} \tau_i/\mu}\right)$ we find an expression for the effective optical parameter of the entire layered system:

$$\gamma_e = \left(\prod_{i=1}^{N} \gamma_i\right) \frac{\sum_{i=1}^{N} \tau_i / \mu}{\sum_{i=1}^{N} \prod_{j \neq i} \gamma_j \, \tau_i / \mu} \tag{B11}$$

If we use expression (B11) to calculate the effective diffuse radiation albedo $\left(\alpha \frac{T_e T_e'}{1-\alpha R_e'}\right)$ and expand each term, it results in the same formula for α_{N2} as is shown in equation (A5). Since both the diffuse and direct albedos of the system are now matched, the total RF_{SW} of the contrail layer system can be calculated by treating it as a single layer with the optical parameter shown in eq. (B11).

B3 Variation of scattering with solar zenith angle

The objective of this section is to assess how the solar zenith angle (θ) affects the potential cooling impact from contrails. In Section 3.1.1 we stated that increasing the solar zenith angle θ also decreases the (net positive) contrail radiative forcing. This is because of an increase in shortwave cooling, since longwave radiation is not affected. Figure B2 shows how the total upscattered fraction of radiation is affected by changes in solar zenith angle. θ varies from 0 (noon) to 90° (sunset), moving anti-clockwise from the top left figure and shown as a black arrow. The dotted horizontal line represents the horizon. F and B represent downward (towards Earth) and upward (back to space) scattering. We assume that 90% of incident radiation is scattered forward, with 10% scattered backwards, representing the high forward scattering fraction of ice particles (high asymmetry parameter *g*). As the solar zenith angle increases, a greater fraction of the forward scattering peak is directed towards space (greater upscatter). This results in an increase cooling effect near sunrise or sunset compared to noon time.

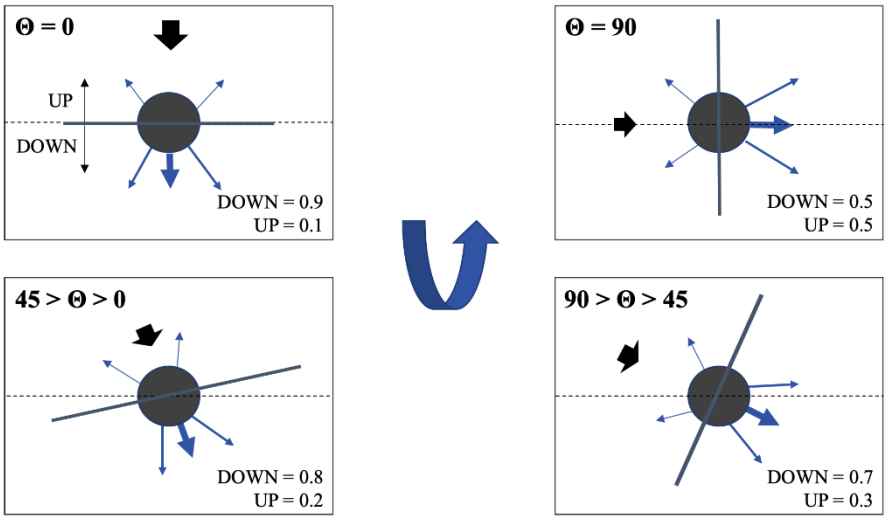

Fig B2. Change in particle reflection when variation in θ (DOWN: downscatter towards Earth; UP: upscatter back to space)

Appendix C: Theoretical explanation of a decrease in cooling when accounting for overlap

This appendix mathematically explains an interesting feature obtained in Section 3.1 related to the effect of two overlapping layers on the shortwave radiation reflectance. This specific result is interesting but does not significantly affect the overall impacts attributable to contrails.

In Section 3.1 we found that, in a small interval of low optical depths and at high solar zenith angles, the amount of radiation reflected when overlapping is higher than the amount of radiation reflected if the two layers were independent, resulting in a higher absolute value of the shortwave RF (Fig. 3a). This is anomalous since two overlapping layers would be expected to reflect less sunlight due to the reduction of covered area.

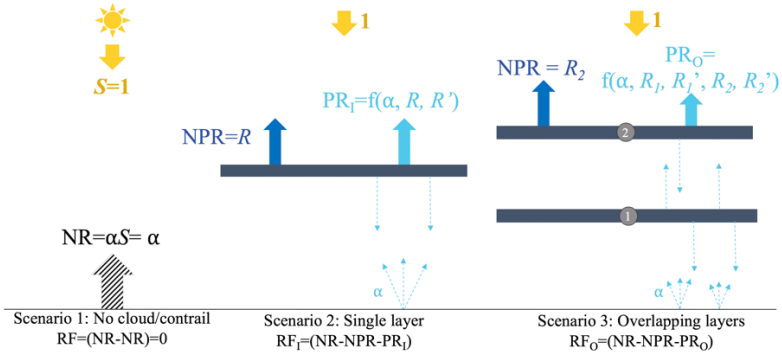

Figure C1 Components of response to a unit of incident light for 3 scenarios: no cloud/contrail, single layer, overlapping layers

In order to explain this, we decompose the fraction of the incident SW radiation flux S reflected by layers of clouds or contrails into non-participating radiation ("NPR") and participating radiation ("PR") (Fig. D1). NPR is the light which is reflected into space from the upper contrail and therefore does not participate in scattering. In turn, it increases with R_c, which rises with optical depth. PR is the remaining outgoing shortwave radiation. Since all light included in PR was reflected or diffused, i.e. it has "participated" in scattering between the layer(s) and the Earth's surface, PR is driven by both direct reflectance R_c and diffused reflectance R_c'. PR decreases with increasing optical depth. Finally, NR is the natural reflectance of light by the surface of the Earth, proportional to its albedo. We note that in the "clear sky" scenario, the total outgoing shortwave radiation is NR = α*S*.

Anomalous case	PR_O-PR_I >$\|RF_{SW,I}\|$ Higher cooling effect by overlapping	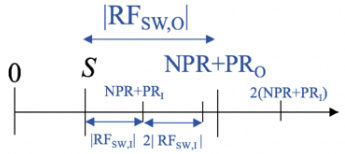
Theoretical case	PR_O-PR_I <$\|RF_{SW,I}\|$ Lower cooling effect by overlapping	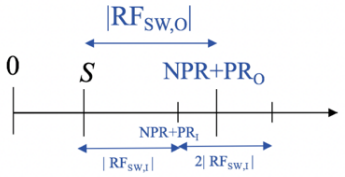

Figure C2. Comparison scheme of reflection components in an overlap (Upper case: increase in cooling; lower case: decrease in cooling)

With this decomposition, we can compute the shortwave RF of a single layer per unit of incoming radiation by comparing the outgoing shortwave radiation with no cloud (α) to that with a cloud layer

(NPR – PR). This yields $RF_{SW,I} = (\alpha - NPR - PR_I)$. For two overlapping layers, the shortwave RF is $RF_{SW,O} = (\alpha - NPR - PRO)$. We then compare this finding to previous work which treats the two layers independently, so that $RF_{SW,2I} = 2 \times (\alpha - NPR - PR_I)$.

First, we can see from the $RF_{SW,2I}$ expression, that the "clear sky" reflection is accounted for twice, which doesn't reflect the reality when two layers overlaps. This indicates that considering two independent layers for calculating RF when these two-layers overlap is not a correct assumption. Additionally, the absolute value of the shortwave RF, or cooling effect, of overlapping contrails will exceed the independently computed cooling effect of two overlapping layers if $(PR_O - PR_I) > |RF_{SW,I}|$, shown schematically in Figure D2. Although PR_O is always higher than PR_I, due to the additional upscatter from the lower layer, this explains why the net cooling is only increased by overlapping (compared to two independent layers) for small optical depths.

As a conclusion, under specific circumstances (low optical depth and solar zenith angle), two contrails overlapping will reflect more radiation (higher cooling effect) than if they were independent, compensating the higher covered area. However, the difference in RF_{SW} for these cases is small enough that it has no noticeable effect on global average values.